~~RESTRICTED~~

Copy 3
RM E50H29

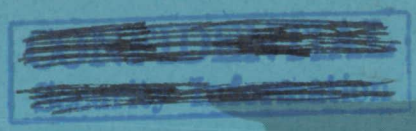

RESEARCH MEMORANDUM

INVESTIGATION OF POWER REQUIREMENTS FOR ICE PREVENTION AND CYCLICAL DE-ICING OF INLET GUIDE VANES WITH INTERNAL ELECTRIC HEATERS

By Uwe von Glahn and Robert E. Blatz

Lewis Flight Propulsion Laboratory
Cleveland, Ohio

NATIONAL ADVISORY COMMITTEE
FOR AERONAUTICS

WASHINGTON
December 1, 1950

~~RESTRICTED~~

NATIONAL ADVISORY COMMITTEE FOR AERONAUTICS

RESEARCH MEMORANDUM

INVESTIGATION OF POWER REQUIREMENTS FOR ICE PREVENTION AND CYCLICAL DE-ICING OF INLET GUIDE VANES WITH INTERNAL ELECTRIC HEATERS

By Uwe von Glahn and Robert E. Blatz

SUMMARY

An investigation was conducted to determine the electric power requirements necessary for ice protection of inlet guide vanes by continuous heating and by cyclical de-icing. Data are presented to show the effect of ambient-air temperature, liquid-water content, air velocity, heat-on period, and cycle times on the power requirements for these two methods of ice protection.

The results showed that for a hypothetical engine using 28 inlet guide vanes under similar icing conditions, cyclical de-icing can provide a total power saving as high as 79 percent over that required for continuous heating. Heat-on periods in the order of 10 seconds with a cycle ratio of about 1:7 resulted in the best over-all performance with respect to total power requirements and aerodynamic losses during the heat-off period.

Power requirements reported herein may be reduced by as much as 25 percent by achieving a more uniform surface-temperature distribution. A parameter in terms of engine mass flow, vane size, vane surface temperature, and the icing conditions ahead of the inlet guide vanes was developed by which an extension of the experimental data to icing conditions and inlet guide vanes other than those investigated was possible.

INTRODUCTION

The desirability for all-weather operation of turbojet aircraft has necessitated extensive research on methods of icing protection for the various engine components. Experience has shown that, in the absence of a compressor-inlet screen, the inlet guide vanes of an axial-flow turbojet engine constitute the most critical component to

be protected from icing. Ice formations on the inlet guide vanes seriously affect engine performance by decreasing the compressor efficiency, by reducing the mass flow through the engine, and by causing large pressure losses at the compressor inlet. These factors, which reduce the net thrust, increase the specific fuel consumption, and increase the tail-pipe temperatures beyond safe operation limits, can render the engine inoperative in a matter of minutes in a heavy icing condition.

Icing in the initial stages of compressor blading in current engines is deemed of secondary importance to inlet-guide-vane icing because icing occurs principally on the leading edges, where ice formations are limited in size by mechanical abrasion due to the close spacing and relative motion between the rotor- and the stator-blade rows.

Ice formations on inlet guide vanes tend to increase rapidly in size at ambient-air temperatures above 10° F. In the temperature range of 10° to 32° F, the ice formations at the leading and the trailing edges tend to mushroom and if the vanes are closely spaced, bridging of the ice formations between adjacent vanes occurs. By use of larger size inlet guide vanes with a greater spacing between vanes, ice bridging between adjacent vanes can be considerably delayed and the icing tolerance of the engine increased. The icing protection of inlet guide vanes may be accomplished by heating the surface of the vanes either by use of hot gas or by electrical means.

An investigation at the NACA Lewis laboratory to determine the electric power requirements for inlet-guide-vane icing protection was conducted on vanes that were twice the size of vanes in current production engines. The increased size was required to provide for adequate instrumentation and is in accordance with current design trends. The investigation was made over a range of icing conditions to determine the minimum electric power requirements for icing protection by continuous heating of the inlet guide vanes. In addition, cyclical de-icing studies were made to determine the possible saving in total power by this system of ice protection over the power required for continuous heating. An analysis is included to extend the experimental results to vane sizes and icing conditions other than those studied.

SYMBOLS

The following symbols are used in this report:

A	surface area, (sq in.)
c_p	specific heat of dry air at constant pressure, (Btu/(lb)($^\circ$F))
$c_{p,w}$	specific heat of wet air at constant pressure, (Btu/(lb)($^\circ$F))
E_M	water-collection efficiency of vane
ΔH	total-pressure loss, (lb/sq ft)
h	convective heat-transfer coefficient, (Btu/(hr)(sq ft)($^\circ$F))
L	latent heat of vaporization, (Btu/lb)
M	rate of water interception, (lb/(hr)(sq ft))
m	liquid-water content, (grams/cu m)
P	power input, (watts)
p	static pressure, (lb/sq ft)
p_v	pressure of saturated water vapor, (lb/sq ft)
Δp	difference between local surface static pressure and free-stream static pressure, (lb/sq ft)
q	dynamic pressure, (lb/sq ft)
S	static-pressure coefficient, $\left[1 - \frac{\Delta p}{q_a}\right]$
s	surface distance, (ft)
T	absolute static temperature, ($^\circ$R)
t	static temperature, ($^\circ$F)
V	air velocity, (ft/sec)
W	mass air flow, (lb/sec)

w weight density of air, (lb/cu ft)

X Hardy's evaporation factor

Z correlation parameter

β local water-impingement efficiency

δ ratio of ambient pressure ahead of vanes to standard NACA ambient sea-level pressure

Subscripts:

a ambient ahead of vanes

av average

cal calculated

d datum

exp experimental

f average of ambient and surface conditions

i initial condition

lam laminar

l local

s surface

st standard

turb turbulent

APPARATUS AND INSTRUMENTATION

The electrically heated guide vane was the center vane of a cascade of five vanes mounted in a special housing in the 6- by 9-foot test section of the icing research tunnel (fig. 1). The walls of the housing and the two guide vanes at each side of the center vane were hollow and gas-heated to prevent icing. The air flow through the housing was regulated by remotely controlled flaps at the exit of the housing.

Each vane had a chord of 2.37 inches and a total span of 6.12 inches, of which 5.90 inches were exposed between the upper and lower walls of the housing. The spacing between vanes was 3.12 inches. Only the electrically heated vane was aluminum with heating elements and guide tubes for thermocouples cast in place. The heating element consisted of Nichrome wire encased in glass-cloth insulation and covered with a copper sheath; the element was in the shape of a hairpin so that both ends emerged from the top of the vane. Four heater circuits were used in the vane investigated and were spaced as shown in figure 2. Each circuit was independently connected to a variable transformer, which permitted selective power input to the four circuits. Power input to the various circuits was measured with a recording wattmeter. An electronic timer was used to regulate the heat-on and heat-off periods for the cyclical de-icing studies. Stainless-steel pilot tubes were positioned in the vane at the time of casting so that thermocouple wires could be inserted. Iron-constantan thermocouples were used and the junction peened flush with the vane surface. The thermocouples were positioned in a chordwise plane (fig. 2) 3 inches from the top of the vane.

The instrumented guide vane was insulated from the housing at both ends in order to minimize heat exchange between the test vane and the gas-heated housing.

Four electrically heated total-pressure tubes and four static-pressure wall taps were installed ahead of the vane cascade to obtain the air velocity through the housing. Three shielded thermocouples were mounted on top of the housing to obtain the tunnel-test-section temperature.

All pressure readings were photographically recorded from multitube manometers and all temperature data were recorded on a flight recorder.

EXPERIMENTAL CONDITIONS AND TECHNIQUES

The average dry-air heat-transfer coefficient and the minimum continuous power input to prevent icing of the electrically heated inlet guide vane were determined at air velocities in the housing ahead of the cascade of approximately 250 and 450 feet per second. All dry-air and icing studies were made with an inlet velocity ratio of 1.0. For the dry-air studies, records were obtained of the power input to each heater, the tunnel air and datum temperatures, the vane-surface temperatures with and without heating, and the air velocity. These data were obtained at a surface-temperature rise of 60° to 70° F when the surface temperature of the inlet guide vane was made as uniform as possible by adjusting the power input to each heater circuit.

In order to determine the minimum continuous power for ice prevention on the vanes at a given icing condition, power inputs to the individual heaters were progressively reduced until a minimum surface temperature of 32° F was reached with as uniform a chordwise surface-temperature distribution as possible. The icing conditions for these studies included a measured liquid-water content of 0.30 to 0.85 gram per cubic meter and a mean effective droplet diameter of 12 to 15 microns; the ambient-air temperature ranged from -35° to 17° F. Data recorded for the continuous heating studies were similar to the dry-air investigations with the addition of the icing condition data.

The investigations of cyclical de-icing power requirements for electrically heated inlet guide vanes were of an exploratory nature with most of the data obtained at an air velocity of about 392 feet per second. One set of data was obtained at 250 feet per second. The icing conditions for these studies were similar to those for the continuous heating studies. The minimum power required for cyclical de-icing was also established by the method used for continuous heating with the additional condition that all ice formations had to be removed at the end of the heat-on time. The heat-on and cycle times investigated were:

Time			Cycle ratio
Heat-on (sec)	Heat-off (sec)	Total cycle (sec)	
10	60	70	1:7
10	120	130	1:13
20	60	80	1:4
20	120	140	1:7
30	60	90	1:3
30	120	150	1:5

The cycle ratio is defined as the ratio of the heat-on time to the total cycle time. Data recorded were similar to those for continuous heating.

RESULTS AND DISCUSSION

The datum surface temperatures measured by the vane thermocouples approximated the datum air temperature measured by the shielded thermocouples mounted above the housing. Similar shielded thermocouples had been calibrated and possessed temperature-recovery factors of 0.83 to

0.87, which varied directly as a function of increasing air-stream Mach number in the range of velocities investigated herein. An average uniform temperature rise over the vane surface of 85 percent of the full adiabatic temperature rise was therefore assumed for all calculations. Temperature-rise data are presented in terms of the vane-surface datum temperature, which is defined as the sum of the ambient-air temperature and the average adiabatic temperature rise on the vane surface. For dry-air conditions, a value of 0.24 was used for c_p in the adiabatic temperature-rise calculations; whereas in wet-air or icing conditions, a value of $c_{p,w}$ that varied with pressure altitude and air temperature was used.

In order to correlate experimental data with theoretical calculations, determination of the pressure distribution over the vane was necessary. A typical pressure distribution in terms of S plotted as a function of s is shown in figure 3. The data shown are for air velocities of 261 and 420 feet per second.

Heat losses caused by end effects were neglected throughout the investigation because the vanes were insulated from the housing.

Continuous Heating of Inlet Guide Vanes

Dry-air heat-transfer evaluation. - Experimental studies were made at several ambient-air temperatures to determine the average dry-air convective heat-transfer coefficient from the vane to the surrounding air. Because the heat flow paths from the first and fourth heaters are relatively long, the power inputs to the first and fourth heater circuits were necessarily high; consequently, the surface-temperature distributions (fig. 4) are nonuniform especially near the trailing edge. Experimental results indicated that for temperature-rise values of 60° to 70° F, temperature variations from the average values of about ±8° F were obtained. The typical temperature distributions over the vane surface, shown in figure 4 as a function of surface distance, were obtained at air velocities of 292 and 457 feet per second.

The temperatures along the convex surface of the vane, as indicated by dashed lines, were estimated from temperatures on the concave surface by assuming one-dimensional heat flow. This assumption also applies to all subsequent surface-temperature data presented herein.

The average experimental convective heat-transfer coefficient was calculated from power input, vane-surface area, and temperature rise as follows:

$$h_{exp,av} = \frac{P}{0.00203A\Delta t}$$

The value of Δt is defined as $t_{s,av}-t_d$. For the surface-temperature distribution and conditions given in figure 4, the $h_{exp,av}$ value at 292 feet per second was 46.4 Btu per (hr)(sq ft)(^{o}F) and at 457 feet per second was 69.5 Btu per (hr)(sq ft)(^{o}F).

Because the vane material used in this investigation was a good conductor, obtaining point convective heat-transfer coefficients experimentally was impossible; consequently only average values were obtained. An analysis was therefore undertaken to obtain a more comprehensive understanding of convective heat transfer from the vane in dry air. By means of theoretical heat-transfer equations for a cylinder and a flat plate (reference 1) and by assuming boundary-layer conditions for the vane, theoretical point convective heat-transfer values were calculated. The pressure-distribution curve, obtained from unpublished data at the Lewis laboratory and given in figure 3, was used to determine local velocities over the vane. The temperature-distribution curves from figure 4 were used in the determination of the point heat-transfer values. The flow conditions assumed over the vane were: The leading-edge convective heat-transfer coefficients were the same as for a cylinder of 0.125-inch diameter; the concave surface of the vane was considered to have a laminar boundary layer; and the convex surface was assumed to have a laminar boundary layer to the point of minimum pressure and a turbulent boundary layer thereafter. The resulting curves of the convective heat-transfer coefficients as a function of surface distance are shown in figure 5. By an integration of the area under the curves, average convective heat-transfer coefficients of 50.0 and 68.4 Btu per (hr)(sq ft)(^{o}F) were obtained for air velocities of 292 and 457 feet per second, respectively. The calculated average values of heat-transfer coefficients are in close agreement with those experimentally obtained and indicate that the assumptions made for the analysis were substantially correct. Further modification of the assumptions to obtain more accurate values appears to be unwarranted because the heat-transfer coefficients in the region where transition from a laminar to a turbulent boundary layer occurs cannot be satisfactorily evaluated.

Wet-air heat-transfer evaluation. - In order to obtain an understanding of the heat-transfer mechanism for icing conditions, an

analysis was made to determine the wet-air heat-transfer coefficients h_{X+M} in terms of local power densities. The analysis used to obtain these coefficients makes use of the wet-air analysis presented in reference 2.

Calculation of the wet-air heat-transfer coefficients required determining the local rate of water impingement on the vane surface. Because neither theoretical nor experimental data are available on water-impingement rates for inlet guide vanes, the following procedure was used to obtain approximate local values of M. The local water-impingement efficiency β was determined by assuming that the water-droplet trajectories were straight-line paths as shown in figure 6(a). The local impingement rate at any point on the vane surface is therefore the ratio of the area contained between adjacent droplet trajectories dy ahead of the vane to the vane surface contained within these trajectories ds. The distribution of β over the blade surface is shown in figure 6(b) as a function of surface distance. This water interception by the vane was based on a water-collection efficiency E_M of 100 percent. Because water droplets do deviate from the air streamlines as a result of the momentum difference between the droplets and the air, E_M is less than 100 percent. On the basis of water trajectory studies reported in reference 3, calculations were made of the collection efficiency for ribbons approximating the projected frontal area and the plan form of the vane. For the air velocities and droplet size used in the present inlet-guide-vane investigation, the collection efficiency of these ribbons was in the order of 80 percent. This value of collection efficiency was assumed for the inlet guide vane. The expression for the water-impingement rate therefore is

$$M = \frac{\beta E_M V_a m}{4.45} = 0.18 V_a m \beta$$

The heat loss from the inlet guide vane caused by evaporation was calculated using Hardy's evaporation factor as given in reference 4. The full evaporation factor was used on all surfaces subject to direct water impingement as indicated by the β values in figure 6(b). Beyond the limit of water impingement on the convex surface, runback was assumed to occur and, based on experimental observations of airfoil sections, an average value of 20 percent of the full evaporation factor was assumed. As in the dry-air analysis, the vane-surface temperatures were maintained as uniform as possible at the minimum total power required to prevent icing. The surface temperatures for two typical cases analyzed are shown in figure 7. The icing conditions for these temperature distributions were: air velocities of 401 and 261 feet per second, ambient-air temperatures of -12° and -5° F, liquid-water

contents of 0.58 and 0.62 gram per cubic meter, and average experimental power densities of 9.3 and 6.4 watts per square inch, respectively.

The same boundary-layer conditions as for the dry-air analysis were initially assumed. Calculations of the local power density as a function of the surface distance were then made (fig. 7) for the icing conditions previously stated. Integration of the area under the curves shown in figure 7 indicated lower total power inputs for icing protection of the vane than were experimentally obtained. The boundary layer assumed on the concave surface was therefore changed to include a turbulent boundary layer over the rearward portion of the inlet guide vane as shown in figure 7. By an adjustment of the amount of vane area assumed to be in the turbulent-flow region, the calculated average value of power density or average wet-air heat-transfer coefficient could be calculated to approach the experimentally obtained average value. The validity of the assumption of a partially turbulent boundary layer on the concave surface has been substantiated in reference 2 and at the Lewis laboratory by unpublished experimental studies of heat transfer from an airfoil in icing conditions, which indicate that a water film on the surface of an airfoil section causes early transition from laminar to turbulent flow.

As indicated in figure 7, the surface temperatures were considerably higher than the theoretical minimum of 32° F. A wet-air analysis based on assumptions similar to those stated previously with respect to impingement, evaporation factor, and boundary-layer considerations indicates that if heaters could be so located as to give a uniform surface temperature of 32° F, power savings of about 25 percent over the power density values shown in figure 7 could be achieved.

Minimum power requirements for ice prevention. - The average minimum total power required per unit area for ice protection of inlet guide vanes is shown in figure 8 as a function of the surface datum temperature. The data shown are for air velocities of approximately 250 and 400 feet per second and a measured liquid-water content ranging from 0.30 to 0.85 gram per cubic meter. The average power density for ice protection of inlet guide vanes increases with a decrease in temperature. Heat-transfer rates and power density values were based on the total surface area of the vane rather than the exposed area as a matter of convenience because the end effects on the vane were neglected.

A tabulation of the icing conditions and pertinent power input values for the continuous heating used in figure 8 are shown in the following table:

V_a (ft/sec)	Measured m (g/cu m)	$t_{s,av}$ (°F)	t_a (°F)	$(P/A)_{av}$ (watts/sq in.)	Total P (watts)	Heater circuit (percent total power)			
						1	2	3	4
236	0.85	35.5	13	2.9	91	22.0	12.1	14.3	51.6
380	.67	37.0	10	4.0	124	29.8	7.2	7.3	55.7
261	.80	40.0	-5	6.4	199	23.6	8.5	7.5	60.4
263	.49	39.0	-5	5.9	183	27.8	6.0	4.9	61.3
401	.58	41.0	-12	9.3	287	24.7	9.8	12.1	53.4
398	.30	41.0	-12	8.8	272	25.4	12.1	9.5	53.0
400	.44	46.0	-35	13.7	424	26.4	10.8	12.0	50.8
240	(a)	41.0	-24	9.7	301	28.5	7.3	7.6	56.6
383	(a)	35.5	17	3.9	122	35.3	7.4	0	57.2

[a]No measurements made.

Typical inlet-guide-vane surface-temperature distributions with continuous heating in an icing condition are shown in figure 9 for surface datum temperatures of 17.5°, -4.5°, and -28° F and an air velocity of approximately 400 feet per second. These temperature distributions indicate that a higher average surface temperature was required to maintain the leading and trailing edges above freezing at low air temperatures than at higher air temperatures. Curves of the variation in the required average surface temperature with surface datum temperature and air velocity are shown in figure 10. From these curves, estimation of the required average surface temperature for ice protection for conditions other than presented herein is possible; these curves, however, apply only to the heating elements and spacing used in this investigation.

Although various power input patterns were investigated, no better power input distribution to the heating elements could be obtained than that shown in figure 11 in which the power to each circuit is presented in percent of total power. Because the trailing edge is effectively a fin, the fourth heater must have a relatively high temperature in order to maintain a 32° F temperature at the trailing edge. Approximately twice as much power is required by the trailing-edge heater than the leading edge where the heater is much closer to the region requiring heat.

Comparison of experimentally and analytically determined minimum power requirements for ice prevention. - An analytical method by which the heating requirements for ice protection of inlet guide vanes can be calculated for vanes and conditions other than those studied herein is presented in the appendix. Although the method has limitations, most operating conditions for inlet guide vanes can be closely calculated. The analysis shows that the experimentally obtained average effective wet-air heat-transfer coefficient can be expressed in terms of the average theoretical turbulent-flow convective heat-transfer coefficient, the full evaporation factor, the rate of water impingement, and a modifying factor. The average power density required for ice prevention can therefore be expressed as

$$\left(\frac{P}{A}\right) = 0.00203(0.62h_{turb}X+M)_{av}(t_s-t_d)$$

where 0.62 is the modifying factor. A series of $(0.62h_{turb}X+M)_{av}$ curves for several liquid-water contents together with the data points given in the preceding table are shown in figure 12 as a function of the correlation parameter Z developed in the appendix. The correlation parameter Z is shown to be a function of engine mass flow, vane size, ambient pressure and temperature ahead of the vanes, vane-surface temperature, and liquid-water content. With a practical installation, a uniform vane-surface temperature may not be attained; consequently the term t_s in the preceding equation may be written $t_{s,av}$. The good agreement between the calculated curves and the experimental data points is evident (fig. 12). Because the evaluation of the average theoretical wet-air heat-transfer coefficient is valid for a large range of operational variables (see appendix), the experimental results obtained herein can be extended to similar guide vanes of different size in other icing conditions. The value of 0.62 for the modifying factor, however, is valid only for vanes having impingement, evaporation, and vane characteristics similar to those investigated.

Cyclical De-Icing of Inlet Guide Vanes

In any application of cyclical de-icing to inlet guide vanes the vanes are heated successively in groups and a large instantaneous power input is required to raise the vane-surface temperature to 32° F during a relatively short heat-on period. An average power requirement can be obtained by dividing the instantaneous power by the total cycle time. By proper cycle timing and grouping of vanes, the product of the average power and the number of vanes in a group is equal to the instantaneous power for a single vane. The total power expended for cyclical de-icing is determined by the product of the instantaneous power per vane and the number of vanes heated during the heat-on period. The

following sections of this report contain the results of a study of the temperature-rise rate and power input required for cyclical de-icing of inlet guide vanes under several icing conditions.

Temperature-rise rate. - Variations of vane-surface temperature at the leading and trailing edges for various heat-on periods with time are shown in figure 13. These data were obtained in an icing condition with an air velocity of about 392 feet per second, a liquid-water content of approximately 0.6 gram per cubic foot, and an ambient-air temperature of -11° F. For a given instantaneous power input to a heated inlet guide vane, the temperature of the blade first rises rapidly and then gradually levels out at the maximum temperature obtainable with the power applied. In cyclical de-icing, the power cut-off for a 10-second heat-on time occurs before the knee of the temperature-rise-rate curve is reached as indicated in figure 13. For a long heat-on time, 30 seconds, the power cut-off occurs well past the knee of the temperature-rise rate (fig. 13). In terms of power input, this temperature characteristic means that large instantaneous power inputs are required for short heat-on periods because the initial temperature-rise rate must be large to reach a specified temperature. For longer heat-on periods, the temperature-rise rate can be reduced (fig. 13) and thereby effect a reduction in instantaneous power input. If the heat-on period is sufficiently long, the continuous heating power requirements are approached. A long heat-on period, however, decreases the cycle ratio, thereby increasing the total power requirements considerably over those required for a short heat-on period (large cycle ratio).

If ice removal occurs on the vane before the power cut-off, the local surface temperature increases (fig. 13(a)). A rapid decrease in temperature occurs whenever partly melted ice formations from an upstream part of the vane pass over a previously de-iced section of the vane (fig. 13(a), 30-second heat-on period). In order to obtain a more complete understanding of the mechanics of ice removal, temperature-rise data were obtained at several chordwise stations including the leading and trailing edges (fig. 14). Complete de-icing of the vane was accomplished after 16 seconds of heating. The icing conditions for these data were similar to those described for figure 13. The power input to the vane was purposely made high to obtain a record of the temperature rise for the period just prior to ice removal and the consequent temperature rise after ice removal. Time increments during which the temperature on the vane surface remained constant near 32° F (stations 1.25, 1.40, 1.70, and 2.42, fig. 14) indicate the melting of ice or the passage of a formation of ice and water from an upstream portion of the vane.

Typical heating and cooling curves at an ambient-air temperature of 11° F are shown in figure 15 for an air velocity of 383 feet per second and a liquid-water content of about 0.8 gram per cubic meter. As shown in this figure, a high ambient-air temperature causes a considerable lag in the vane cooling rate after ice removal. Freezing of the impinging water on the vane is shown by the relatively constant temperature for the initial 5 seconds of the cooling period. The constant temperature is caused by heat storage in the vane from the heating cycle and the release of the latent heat from the water freezing on the vane surface. These effects were not observed at lower ambient-air temperatures because the large temperature differential between the surface and the ambient air caused a rapid dissipation of the latent heat released from the impinging water.

Power input for cyclical de-icing. - The experimental data showed that the power input per heating circuit with cyclical de-icing was only slightly higher than the power used with continuous heating except near the leading edge. As a basis for comparison, the ratio of power inputs to leading-edge heaters for cyclical de-icing and for continuous heating is plotted in figure 16 as a function of the heat-on period. As the heat-on period was increased and the power input reduced, the power of the leading-edge heater approached the power required for continuous heating. For short heat-on periods, the power input ratio of the leading-edge heater increased rapidly and reached a value of about 2.5 for a heat-on period of 10 seconds. For shorter heat-on periods, the power input to the leading-edge heater rapidly approaches the burnout limit of the heating element.

The bar graph in figure 17 illustrates the percent of total power input to each heater circuit for continuous and cyclical de-icing. The ratio of the leading- to trailing-edge power input for cyclical de-icing is approximately unity, whereas for continuous heating the ratio approached a value of 2.0. In the evaluation of figure 17, the total power input per vane is higher for cyclical de-icing than for continuous heating.

The instantaneous power density in watts per square inch required for cyclical de-icing is shown in figure 18 as a function of vane-surface datum temperature for various cycle times, air velocities of 240 and 390 feet per second, and liquid-water content ranging from 0.3 to 0.8 gram per cubic meter. The relation between the power density and surface datum temperature is approximately linear for each heat-on period investigated. Although the data are limited, the effect of air velocity on the power input required for cyclical de-icing appears to be of secondary importance. The insulation effects or heat capacity of

the ice formation, however, are of primary importance and heat conduction rather than heat convection must be considered for cyclical de-icing. In the results presented herein, evaluating the effect of altitude on the cyclical de-icing performance of the vane was not possible. It can be surmized, however, that, as the altitude increases and the air forces tending to shed the ice during the heat-on period are decreased, more heat than indicated in figure 18 will be required to provide a greater water film under the ice cap to facilitate ice removal.

A comparison of figures 8 and 18 shows that as the surface datum temperature decreases, the ratio of the average power densities between cyclical de-icing and continuous heating required for ice protection increases. This increase is caused by the evaporation factor X, which influences heating requirements much more during continuous heating than during cyclical de-icing.

From the curves presented in figures 13 to 18, determination of total power requirements and of power inputs to each heater circuit for cycle times and for icing conditions other than those studied herein is possible.

Practical aspects of cyclical heating. - The selection of a heating cycle for a particular engine depends on the following: the total number of inlet guide vanes to be heated at any one time, the design icing condition, and the total instantaneous power available for de-icing. The instantaneous power allowable per vane is determined by the temperature limits of the heating elements. Destruction tests of the heating elements similar to those used in this investigation showed a maximum power input of 40 watts per linear inch with nominal metal temperatures could be attained. For design purposes, a value of not more than 25 to 30 watts per linear inch should be used.

Inappreciable differences in power requirements for cyclical de-icing were observed for a change in heat-off periods under similar heat-on periods and icing conditions. It can be assumed therefore that the differences in the magnitude of ice formations occurring in 60 and 120 seconds of icing with the water contents used in the investigation do not seriously affect the heat requirements for cyclical de-icing. The magnitude of the ice formations must, however, be considered because of mass flow and pressure losses associated with various icing periods.

The rate at which the ram pressure decreases with time in an icing condition is shown in figure 19. These data are reported in reference 5 and were obtained at air velocities of 260 and 420 feet per second, liquid-water contents of 0.6 to 0.8 gram per cubic meter, and ambient-air temperatures of -3° to 18° F. The data indicate that at the higher ambient-air temperatures the rate of pressure loss is considerably greater than at the lower ambient-air temperatures. With respect to cyclical de-icing, a short heat-off period of about 60 seconds therefore appears to be more desirable than longer periods in the order of 120 seconds. Photographs of typical ice formations on an inlet guide vane are shown in figure 20 for an air velocity of 400 feet per second. The icing conditions for the ice formations shown in these photographs were a liquid-water content ranging from 0.4 to 0.85 gram per cubic meter with ambient-air temperatures ranging from -31° to 10° F. The large ice formations on the leading and trailing edges for the 120-second icing period were similar to those causing the large pressure losses shown in figure 19. These losses were primarily caused by the reduction in the free flow area by the ice formations between adjacent vanes.

For a given power input per vane and heat-on period but varying heat-off periods, the greatest power saving is accomplished with the longest heat-off period because the least number of vanes are heated at any one instant. As an illustrative example, a hypothetical engine is assumed to have 28 vanes of the size and type investigated herein. Because fractional parts of a vane cannot be heated, the number of blades heated at any one time is a number divisible into 28, such as 1, 2, 4, 7, 14, or 28. The first and the last two numbers are ruled out on the basis of too long a heat-off period and too short a heat-off period, respectively. If four vanes are to be heated (1:7 cycle ratio), a 20 - 120 second or a 10 - 60 second cycle may be used. If 7 vanes are to be heated at a given instant, a 20 - 60 second cycle may be used. The three cycles that can be used are shown in figure 21 wherein the ratio of total cycle period to heat-on period is plotted as a function of total power required for cyclical de-icing of the heated vanes. The icing conditions assumed for these cycle periods were liquid-water content of 0.6 gram per cubic meter, air velocity of 400 feet per second, and ambient-air temperature of -11° F. Also given in figure 21 is the power required for continuous heating at a cycle ratio 1:1 (7800 watts or 9.0 watts per square inch). For a 20-second heat-on period and an instantaneous power input of 330 watts per vane, the calculations indicate that a total power of 1320 watts is required for a heat-off period of 120 seconds and 2310 watts is required for a heat-off period of 60 seconds. For similar cycle ratios (1:7) in which a 20 - 120 second and 10 - 60 second cycle are used, the 20 - 120 second cycle provided only a small saving in total

power. Although the 10 - 60 cycle requires a greater instantaneous power input per vane (412 watts), the total power used was only 1650 watts or 25 percent greater than the total power required for the 20 - 120 second cycle. The utilization of a 10 - 60 second cycle for the icing conditions given in figure 21 will achieve a reduction of 79 percent in the total power required for ice protection with continuous heating. The saving of power for the 20 - 120 second cycle is exceeded by the loss in pressure that would be obtained at higher ambient-air temperatures as illustrated in figure 19. From a consideration of pressure and mass-flow losses that might be incurred, the 10 - 60 second cycle appears to hold the greatest advantages for the hypothetical engine configuration. A shorter heat-on period will provide a more efficient use of the power input; the burnout limit of the heater, however, will limit the heat-on time as previously stated.

CONCLUDING REMARKS

Although the compressor blading on current axial-flow turbojet engines is subject to icing primarily on the leading edges, the use of larger inlet guide vanes and consequently larger spacing between vanes may affect compressor-blade icing characteristics. The possibility exists that larger vane spacing will result in ice accretions on the concave surface of the first-stage rotor and stator blades. Should these ice accretions prove sufficiently severe to affect engine performance, these engine components must also be protected. The analysis presented herein for minimum power requirements with continuous heating of inlet guide vanes may be applied to the compressor blading.

The use of materials other than aluminum for inlet guide vanes will in all probability necessitate an increase in the average surface temperature and power input required for ice protection if heating elements are used similar to those in the present study. Because the leading and trailing edges are heated by conduction from the nearest heating elements, the use of lower conductivity metals will require larger power inputs to these heaters and will result in a greater heat dissipation at the center portions of the vane. Relocation of heating elements at the leading and trailing edges should reduce the power required for icing protection even if the metal used has low conductivity properties. It is therefore recommended that heating elements, regardless of the type used, should be located close to the leading and trailing edges provided that such heater installations do not adversely affect the aerodynamic characteristics of the vanes.

SUMMARY OF RESULTS

From a study of the electric power requirements necessary for ice protection of inlet guide vanes by continuous heating and by cyclical de-icing, the following results were obtained:

1. The average power requirement per inlet guide vane per cycle is in the order of 79 percent less than that required for continuous heating under the same conditions: namely, air velocity ahead of the vane, 400 feet per second; ambient-air temperature, -11° F; liquid-water content, approximately 0.6 gram per cubic meter; heat-on time, 10 seconds; and cycle ratio 1:7.

2. Cycle periods of 10 or less seconds heat-on and 60 seconds heat-off result in the best over-all performance with respect to total power input required for icing protection and aerodynamic losses during the heat-off period.

3. For conditions similar to those given in the first result, the electric power requirements for a hypothetical engine utilizing continuous heating for the 28 inlet guide vanes with a total vane area of 865 square inches was 7800 watts (9.0 watts/sq in.), whereas under the same conditions cyclical de-icing required only 1650 watts. Because a uniform surface temperature could not be fully attained on the inlet guide vane investigated, the continuous requirement is approximately 25 percent higher than would be required for a uniform surface temperature of 32° F.

4. A parameter was developed in terms of the engine mass flow, vane size, ambient pressure and temperature ahead of the inlet guide vanes, surface temperature, and liquid-water content that permits a determination of power requirements for ice prevention beyond the limits of the experimental studies. The experimental values of power required for ice prevention of inlet guide vanes coincide closely with values calculated using this parameter.

Lewis Flight Propulsion Laboratory,
National Advisory Committee for Aeronautics,
Cleveland, Ohio.

APPENDIX - APPLICATION OF RESULTS TO OTHER VANES AND ICING CONDITIONS

Because the experimental data presented herein covers only a limited range of operating conditions and a single vane size, extension of the experimental results by analytical means is desirable. In a dry-air condition, the heat transfer from a surface can readily be expressed by the equations given in reference 2 for laminar or turbulent boundary-layer conditions. It remains, however, to determine whether the wet-air heat-transfer coefficient (hX+M) can be expressed by a parameter as a single curve. Previous wet-air analyses (reference 2) as well as the studies reported herein indicate that much of the heat transfer from a heated surface in the presence of a water film or water runback on the surface occurs under transition and turbulent boundary-layer conditions. An analysis was therefore undertaken to evaluate the average heat-transfer coefficient from a heated inlet guide vane for which average values of h_{turb}, X, and M were calculated and a parameter was developed to correlate these values on a single curve.

The variables considered for this analysis were ambient-air pressure, ambient-air temperature, air velocity, vane-surface temperature, vane size, and liquid-water content. The air-stream conditions were obtained for a station just ahead of the inlet guide vanes and were not necessarily ambient conditions. The equation used to obtain average values for turbulent convective heat-transfer coefficient (reference 1) can be expressed as

$$h_{turb,av} = 0.64(T_f)^{0.3}\left(\frac{wV_{l,av}}{s^{0.25}}\right)^{0.8} \tag{1}$$

In order to account for the loss in heat by evaporation, Hardy's evaporation factor X (reference 4) was used in the following form:

$$X = 1 + \frac{0.622L}{c_p \delta p_{a,st}}\left(\frac{p_{v,s}-p_{v,d}}{t_s-t_d}\right) \tag{2}$$

The rate of water impingement is

$$M = \frac{\beta E_M V_a m}{4.45} \tag{3}$$

The ranges of the various variables investigated were as follows: δ, 0.2 to 1.0; T_a, 440° and 480° R; $V_{l,av}$, 200 to 600 feet per second;

s, 0.1 to 0.4 feet; t_s, 35° to 100° F; and m, 0 and 1.15 grams per cubic meter. A plot of the values of the average wet-air heat-transfer coefficient $(h_{turb}{}^{X+M})_{av}$ for the range of variables listed against $wV_{l,av}$ on logarithmic coordinates results in a series of parallel straight lines (fig. 22(a)). The calculated points are based on constant air and surface temperatures. Similar curves are obtained for each air and surface temperature considered. The effect of vane size, as represented by the average surface distance s, was determined by plotting values of $(h_{turb}{}^{X+M})_{av}$ for constant values of δ, $wV_{l,av}$, and t_s against s. It was determined that $(h_{turb}{}^{X+M})_{av}$ varied as $s^{-0.2}$. In figure 22(b), the wet-air heat-transfer coefficient is plotted as a function of $wV_{l,av}/s^{0.2}$ for two absolute ambient-air temperatures, three δ values, and a uniform surface temperature. The next step in the analysis was to determine the variation of $(h_{turb}{}^{X+M})_{av}$ with absolute ambient-air temperature T_a. When $(h_{turb}{}^{X+M})_{av}$ is plotted against T_a at constant values of $wV_{l,av}/s^{0.2}$, δ, and t_s, the data fall along approximately parallel lines having a slope of 3. For convenience of calculation, $(T_a/100)^3$ is used in place of $T_a{}^3$ in correlating data points at different ambient-air temperatures. A typical plot of $(h_{turb}{}^{X+M})_{av}$ is shown in figure 22(c) as a function of $(wV_{l,av}/s^{0.2})(T_a/100)^3$ for a surface temperature of 40° F. In a similar manner, $(h_{turb}{}^{X+M})_{av}$ is found to vary as the -0.61 to -0.65 power of δ and the -0.63 power is used in the parameter being developed. Thus far, $(h_{turb}{}^{X+M})_{av}$ correlates to a single curve when plotted against the parameter $(wV_{l,av}/s^{0.2})(T_a/100)^3(1/\delta^{0.63})$ at uniform surface temperatures t_s. Figure 22(d) is a typical plot for a surface temperature of 40° F. Similar curves were developed for surface temperatures of 35° and 45° F. Check points were also calculated for surface temperatures of 70° and 100° F. The variation of surface temperature with the parameter shown in figure 22(d) was determined to be a straight line relation when plotted on a semilogarithmic scale. The equation of this curve was found to be a function of $(3.2)^{\frac{T_s}{100}}$. The final correlation parameter Z was determined as

$$Z = \left(\frac{wV_{l,av}}{s^{0.2}}\right)\left(\frac{T_a}{100}\right)^3\left(\frac{1}{\delta^{0.63}}\right)\left[(3.2)^{\frac{T_s}{100}}\right] \qquad (4)$$

and is shown plotted as a function of $(h_{turb}X+M)_{av}$ in figure 22(e). Limitations to the correlation parameter are as follows: At surface temperatures of 100° F, the parameter is valid only at δ values near 1.0; and at surface temperatures of 70° F, the limiting δ value is approximately 0.4. These limiting values are necessary because of the rapid increase in vapor pressure and the evaporation factor X for a combination of high surface temperatures and high altitudes. At surface temperatures of 30° to 50° F, the parameter is valid for δ values as low as 0.2. Because of the water-impingement characteristics on the vane assumed in the analysis, the average wet-air heat-transfer coefficient is conveniently expressed in the form of $(h_{turb}X)_{av}$ (fig. 22(f)), to which the rate of water impingement M can then be added for the particular vane and icing condition under consideration. The scatter of the points shown in figures 22(e) and 22(f) are in the order of ±5 percent. The equation for the upper curve in figure 22(f) can be expressed as

$$(h_{turb}X)_{av} = 0.000554(Z)^{0.88} \tag{5}$$

where Z is the correlation parameter. It has therefore been demonstrated that for the usual range of icing and operating conditions for inlet guide vanes, average wet-air heat-transfer coefficient can be correlated on a single curve, with a constant liquid-water content.

The wet-air analysis, previously discussed in the text, indicated that the inlet guide vanes studied did not operate with a fully turbulent boundary layer nor did a portion of the surface experience the effect of the full evaporation factor X. The values of $(h_{turb}X+M)_{av}$ given in figures 22(e) and 22(f) as a function of Z must therefore be modified to apply to a practical operating condition. An analysis of the experimental data indicates that a series of curves can be calculated by multiplying $(h_{turb}X)_{av}$ by 0.62 and adding M, which corresponds to a given water content, from equation (3); this series of curves closely correlates the calculated average wet-air heat-transfer coefficient with experimental data. The term $(0.62h_{turb}X)_{av}$ can also be expressed as $0.000343(Z)^{0.88}$. These values will be obtained only if the impingement, evaporation, and vane characteristics are similar to those studied. For example, because hot-gas-heated inlet guide vanes have high surface temperatures, the impinged water may evaporate before it reaches the trailing edge and leave part of the surface completely dry; in this case, the modifying factor is less than 0.62, varying with the amount of completely dry surface. For cases in which $E_M \neq 0.8$, the

term $(0.62h_{turb}X)_{av}$ still applies as a base and curves for various water contents can be obtained by evaluating new M values and adding these values to $(0.62h_{turb}X)_{av}$ or to the $0.000343(Z)^{0.88}$ value. If the average local velocity over both sides of the vane approaches that of the free-stream velocity, as was the case in the present investigation where $V_{l,av} = 1.041V_a$, $wV_{l,av}$ may be written as $k' W/A$. The value of k' is the velocity ratio $V_{l,av}/V_a$ and W/A is the mass flow per unit area through the cascade. In the mass flow form, the correlation parameter Z is more convenient to the designers of turbojet-engine ice-prevention systems in that the mass flow of the engine is known, but the velocity ahead of the guide vanes may not be readily obtainable. From the average effective wet-air heat-transfer coefficient, the average power required for ice prevention for any icing condition is then obtained from the following equation:

$$\frac{P}{0.00203(t_s-t_d)A} = (0.62h_{turb}X+M)_{av} = \left[0.000343(Z)^{0.88} + M_{av}\right] \qquad (6)$$

REFERENCES

1. Boelter, L. M. K., Martinelli, R. C., Romie, F. E., and Morrin, E. H.: An Investigation of Aircraft Heaters. XVIII - A Design Manual for Exhaust Gas and Air Heat Exchangers. NACA ARR 5A06, 1945.

2. Neel, Carr B., Jr., Bergrun, Norman R., Jukoff, David, and Schlaff, Bernard A.: The Calculation of the Heat Required for Wing Thermal Ice Prevention in Specified Icing Conditions. NACA TN 1472, 1947.

3. Langmuir, Irving, and Blodgett, Katherine B.: A Mathematical Investigation of Water Droplet Trajectories. Tech. Rep. No. 5418, Air Materiel Command, AAF, Feb. 19, 1946. (Contract No. W-33-038-ac-9151 with Gen. Elec. Co.) (Available from U.S. Dept. Commerce as PB No. 27565.)

4. Gray, V. H., and Campbell, R. G.: A Method for Estimating Heat Requirements for Ice Prevention on Gas-Heated Hollow Propeller Blades. NACA TN 1494, 1947.

5. Gray, Vernon H., and Bowden, Dean T.: Icing Characteristics and Anti-Icing Heat Requirements for Hollow and Internally Modified Gas-Heated Inlet Guide Vanes. NACA RM E50I08, 1950.

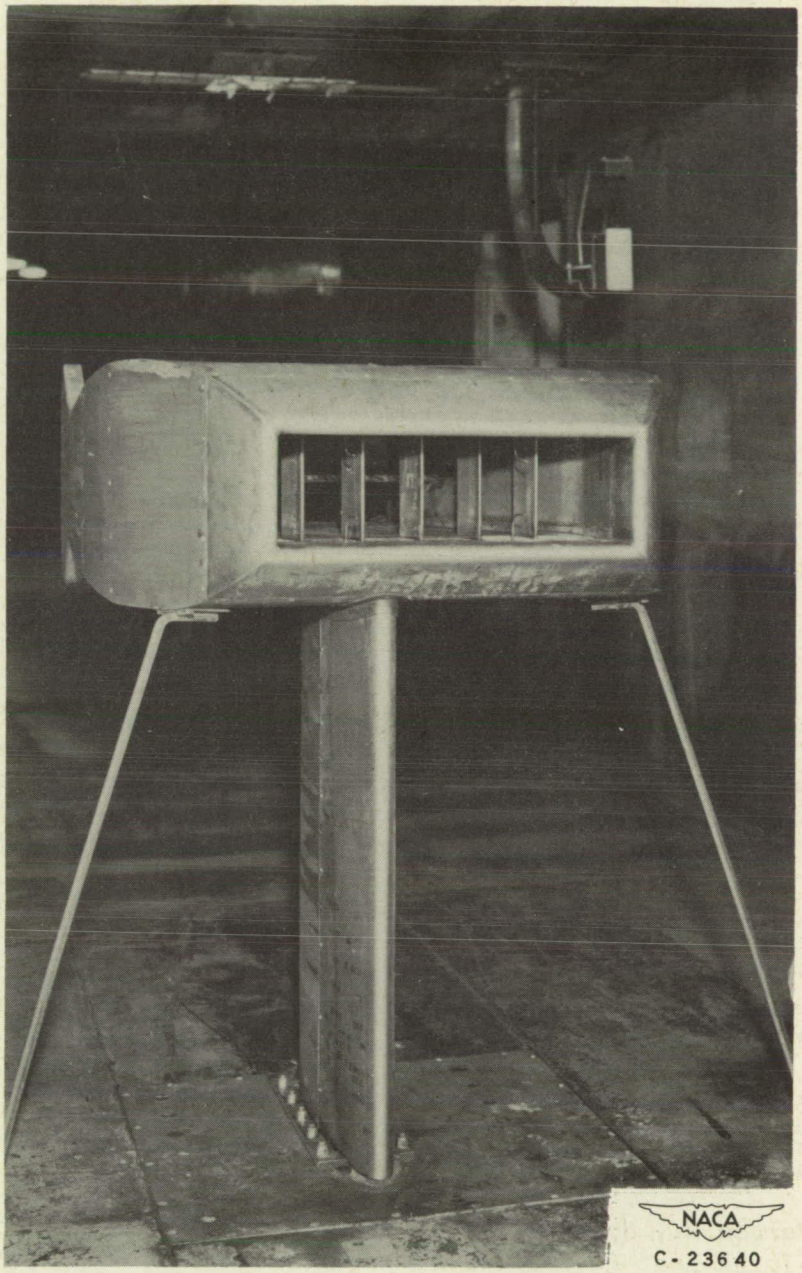

Figure 1. - Inlet-guide-vane installation in icing research tunnel.

Page intentionally left blank

Page intentionally left blank

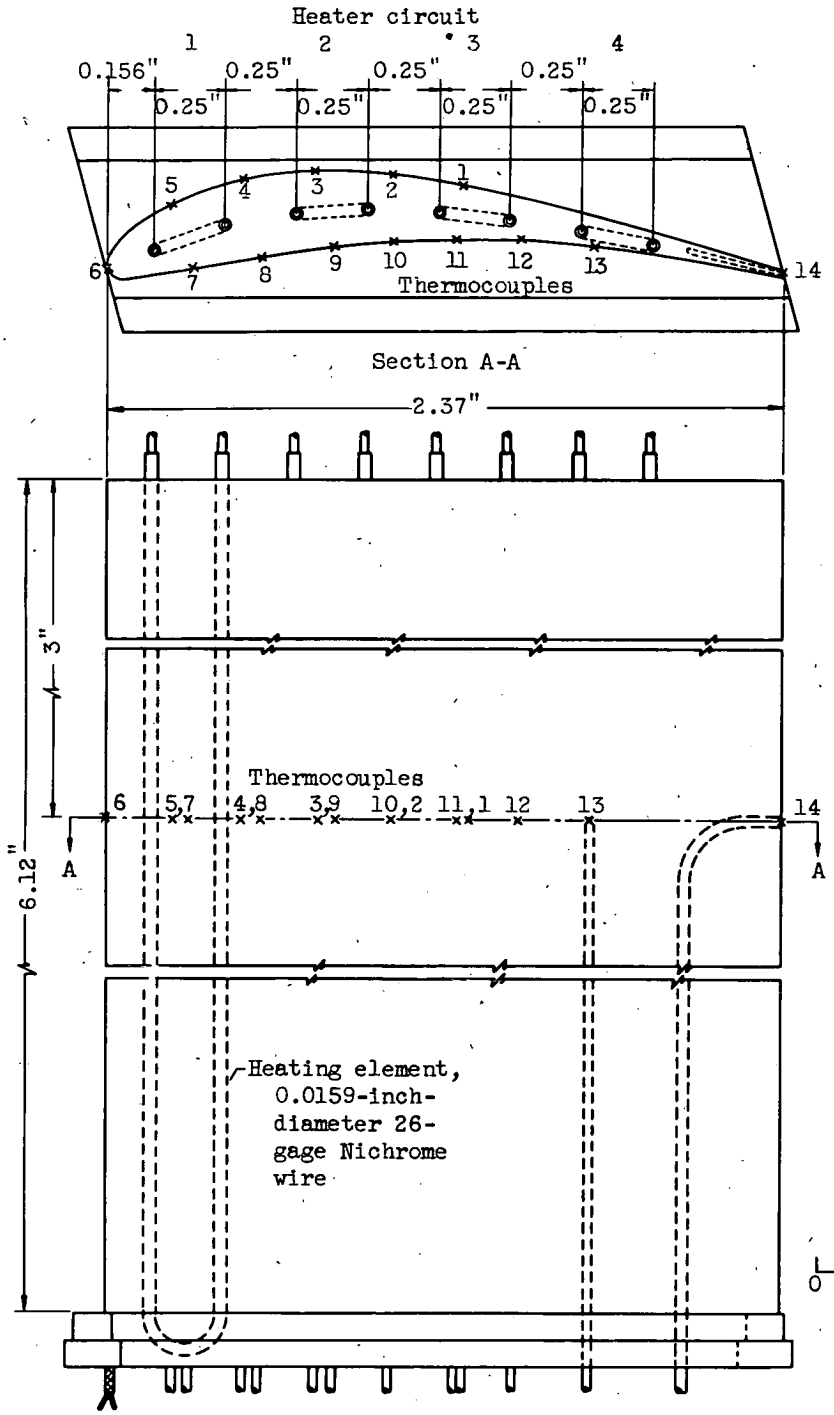

Thermocouple	Location (surface distance from L.E.) (in.)
1	1.408
2	1.142
3	.876
4	.610
5	.344
6	L.E.
7	.312
8	.562
9	.812
10	1.031
11	1.250
12	1.469
13	1.735
14	T.E.

Figure 2. - Construction details of electrically heated inlet guide vane showing location of heater circuits and surface thermocouples.

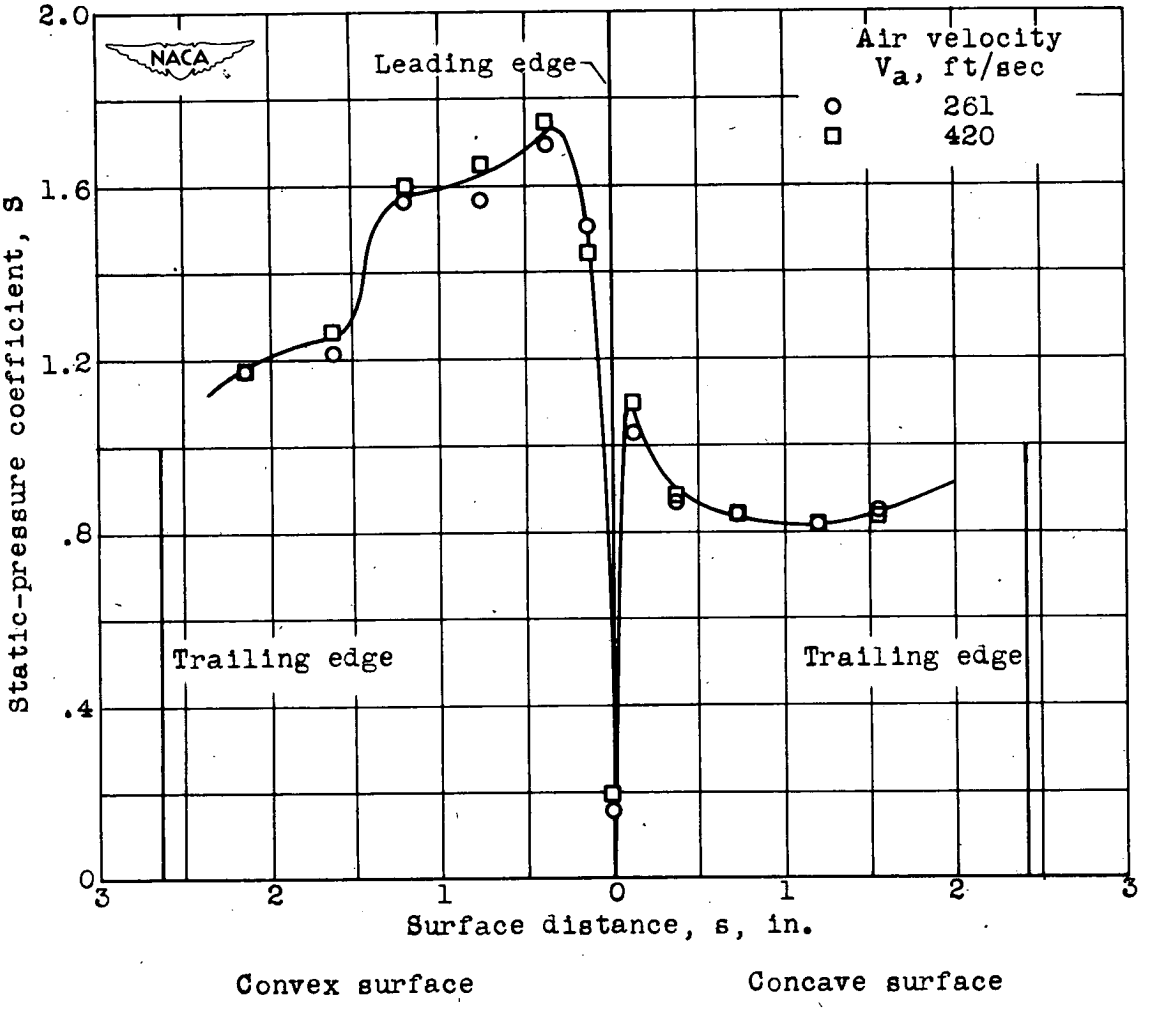

Figure 3. - Variation of static-pressure coefficient with inlet-guide-vane surface distance.

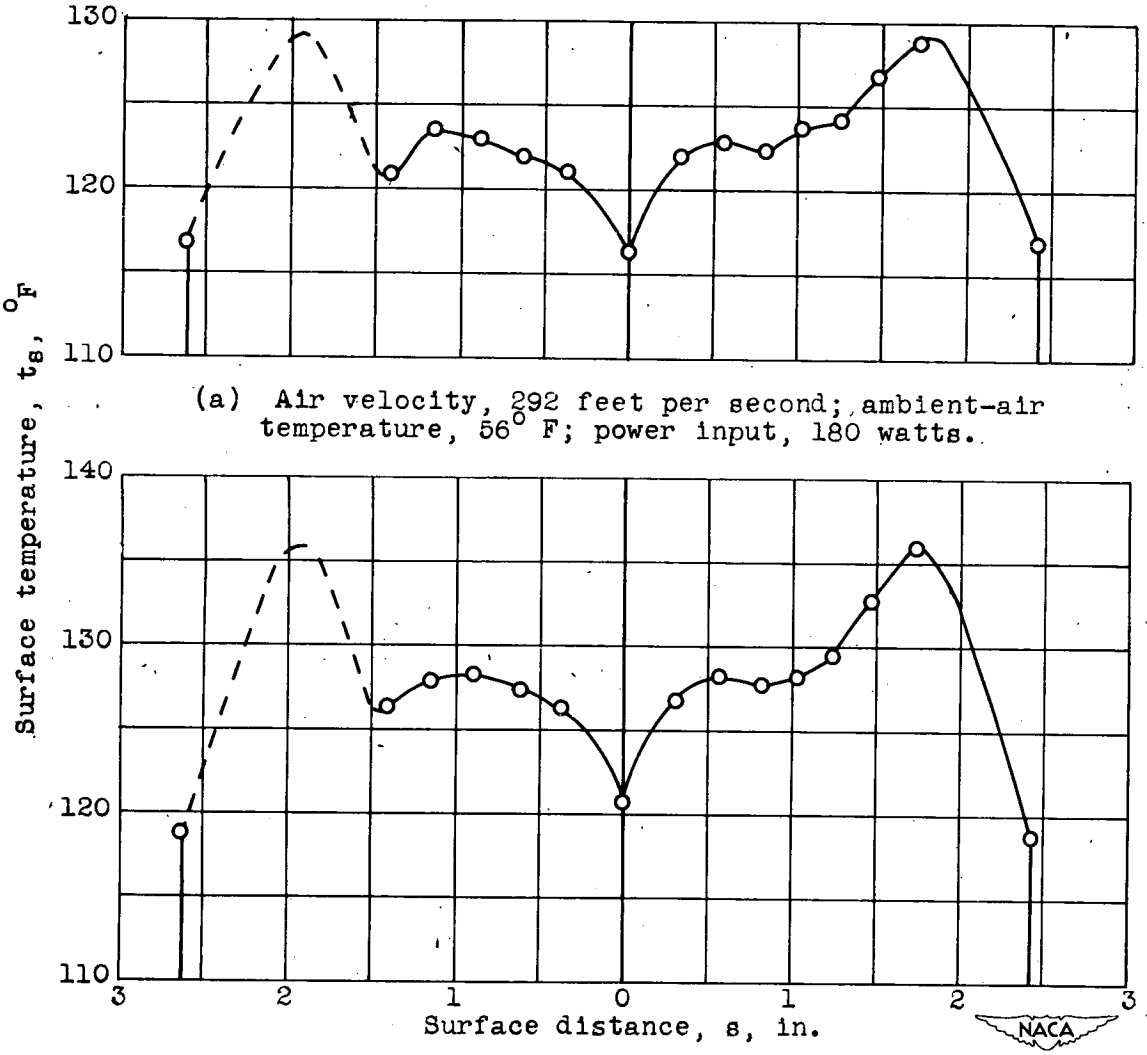

(b) Air velocity, 457 feet per second; ambient-air temperature, 50° F; power input, 265 watts.

Figure 4. - Typical vane-surface-temperature distribution in dry air with continuous heating as function of inlet-guide-vane surface distance.

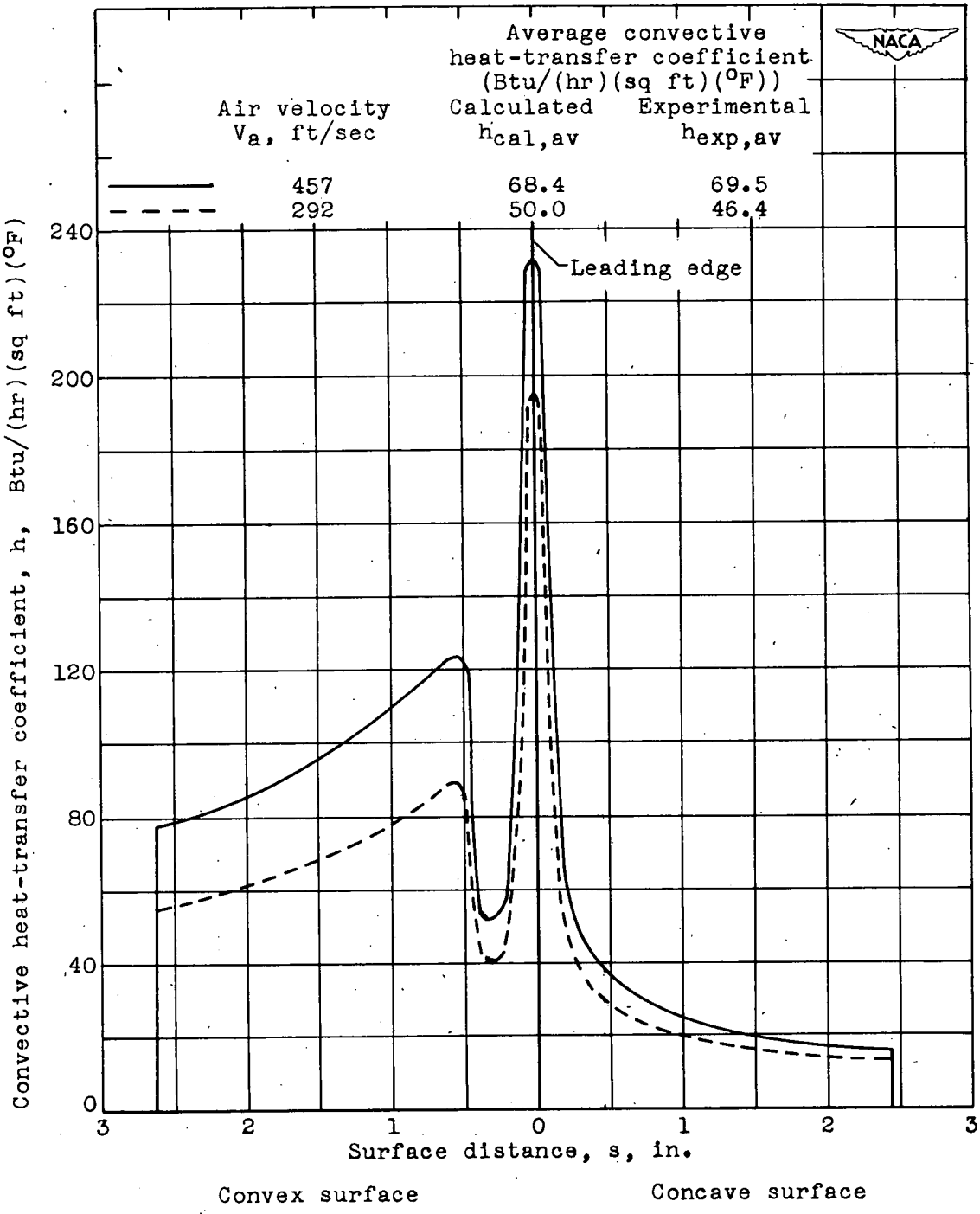

Figure 5. - Calculated convective heat-transfer coefficient in dry air with continuous heating as function of inlet-guide-vane surface distance.

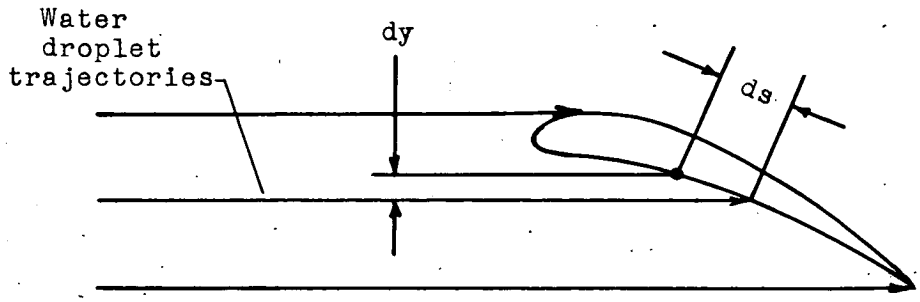

$$\beta = \frac{dy}{ds}$$

(a) Vane droplet trajectory assumptions.

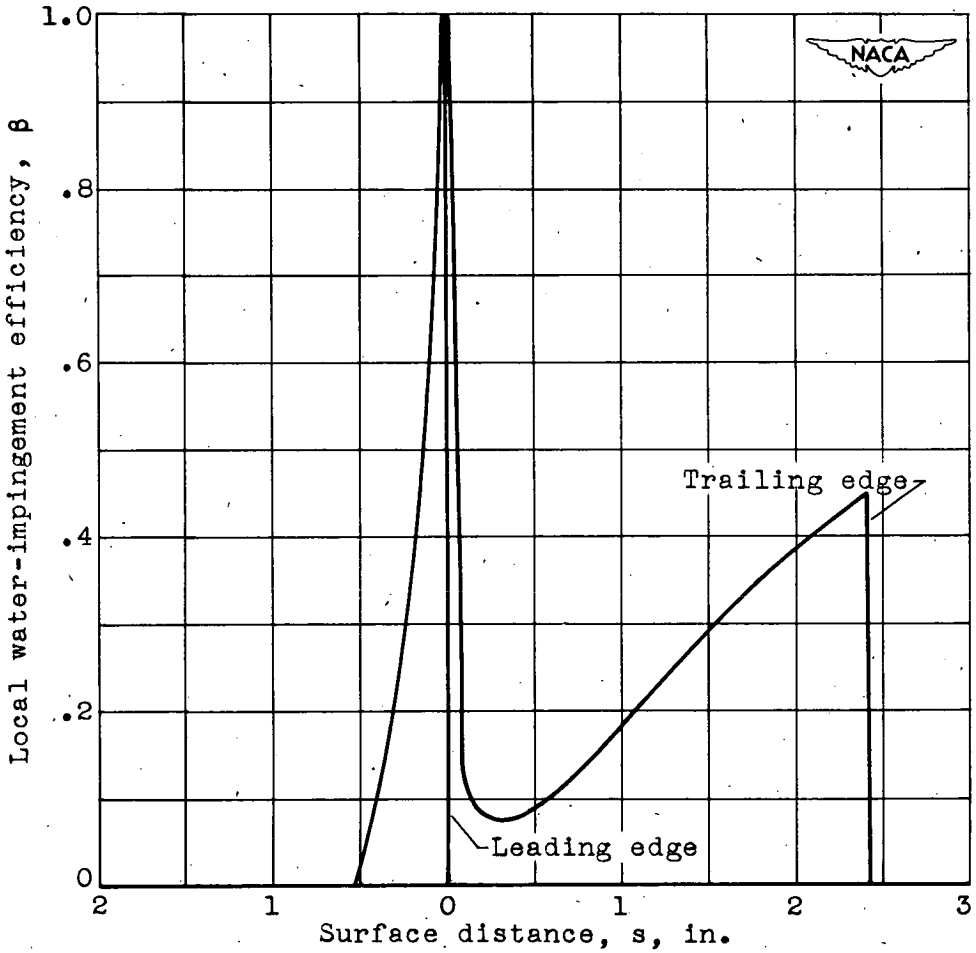

(b) Calculated water deposition over inlet guide vane.

Figure 6. - Calculated variation of local water-impingement efficiency over inlet-guide-vane surface. Collection efficiency E_M, 100 percent.

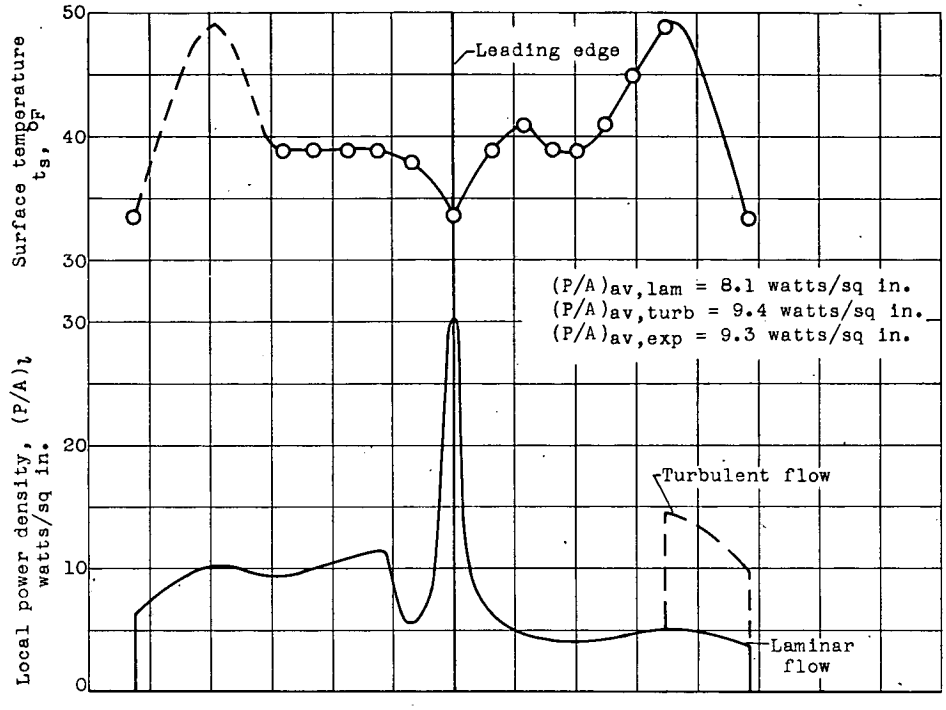

(a) Air velocity, 401 feet per second; ambient-air temperature, -12° F.

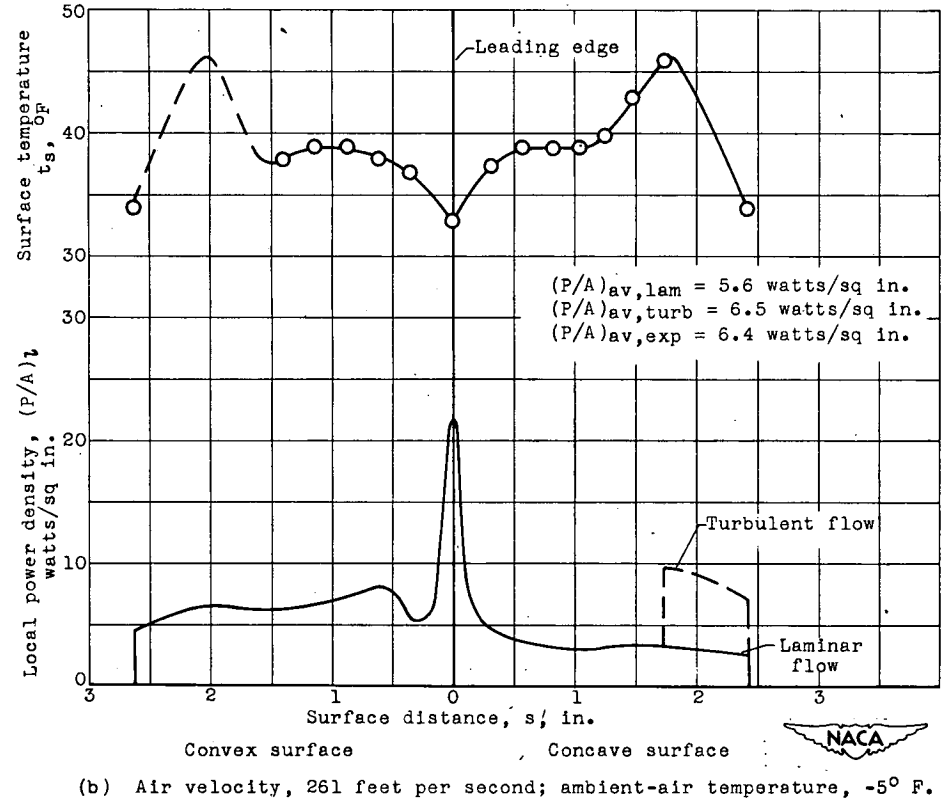

(b) Air velocity, 261 feet per second; ambient-air temperature, -5° F.

Figure 7. - Typical wet-air analysis of local power density over inlet-guide-vane surface. Liquid-water content, approximately 0.6 gram per cubic meter.

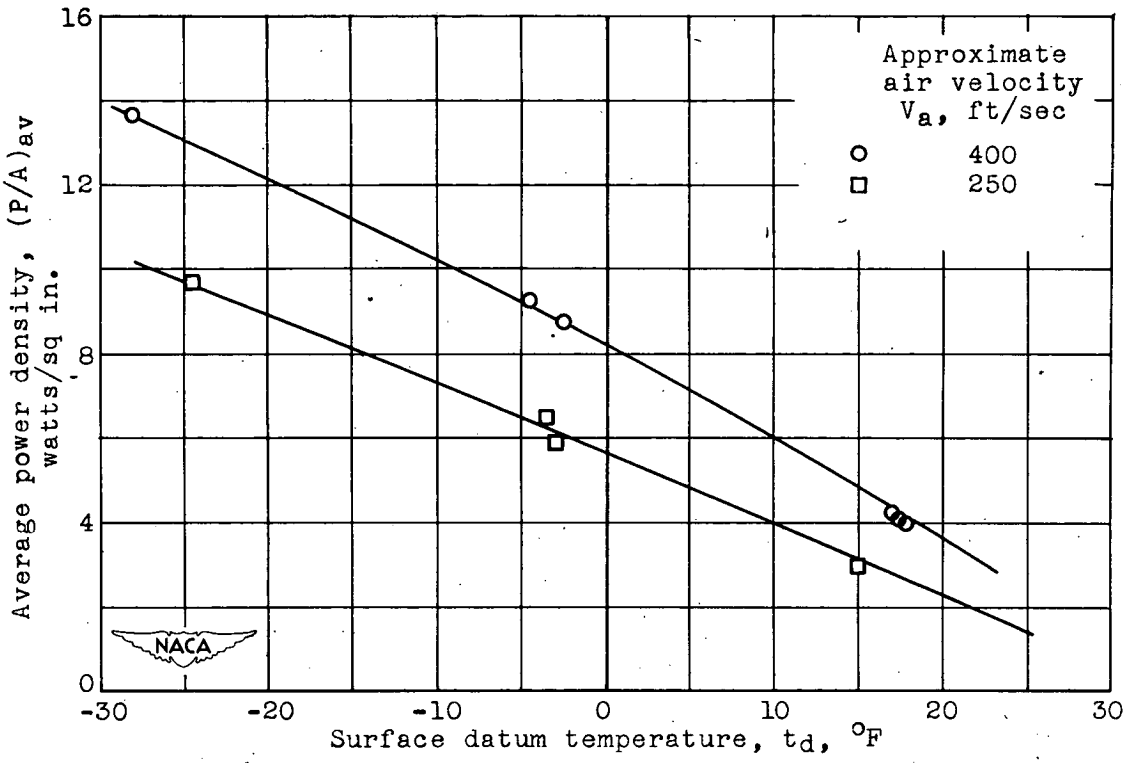

Figure 8. - Minimum power requirements for ice prevention with continuous heating as function of inlet-guide-vane surface datum temperature. Liquid-water content, 0.30 to 0.85 gram per cubic meter.

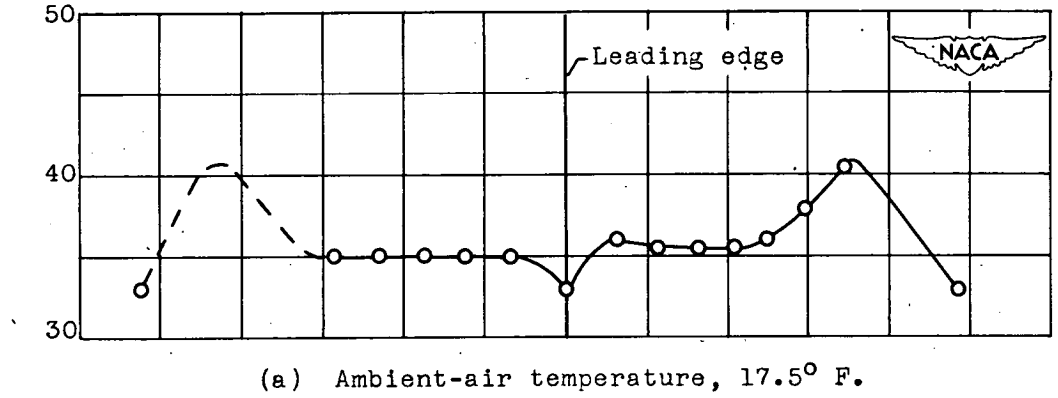

(a) Ambient-air temperature, 17.5° F.

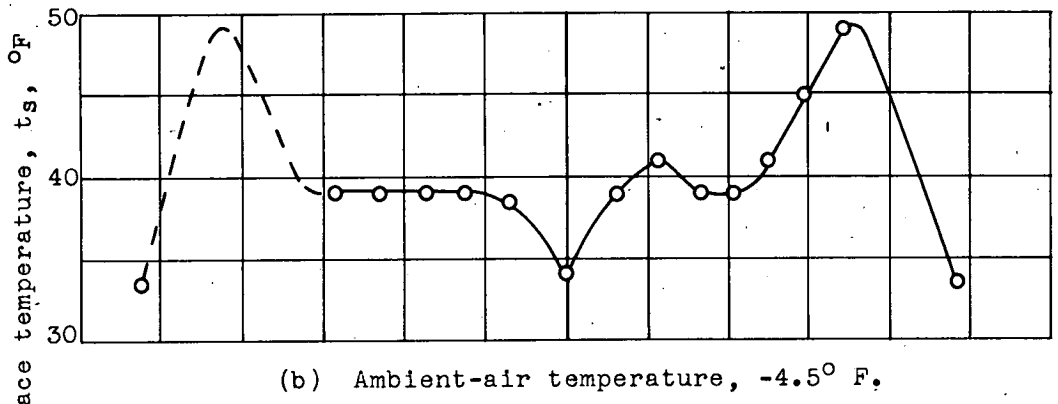

(b) Ambient-air temperature, -4.5° F.

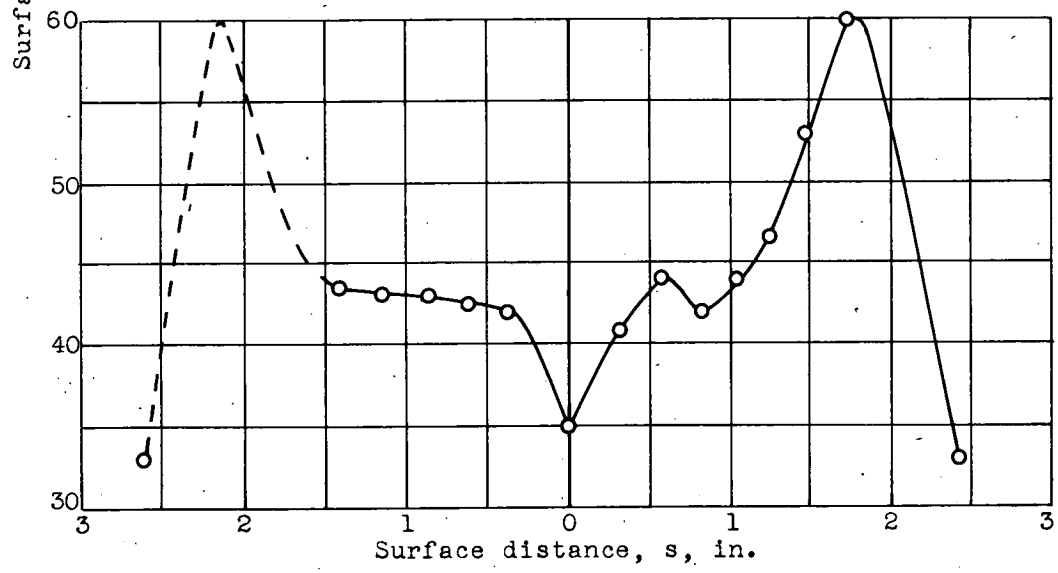

(c) Ambient-air temperature, -28° F.

Figure 9. - Variation of surface-temperature distribution with continuous heating as function of inlet-guide-vane surface distance for several surface datum temperatures. Air velocity, 400 feet per second; liquid-water content, 0.4 to 0.7 gram per cubic meter.

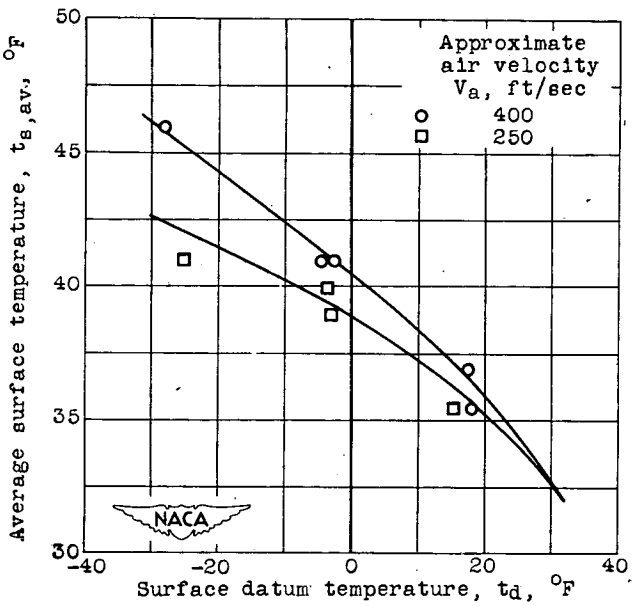

Figure 10. - Variation of average surface temperature for continuous heating with inlet-guide-vane surface datum temperature. Liquid-water content, 0.30 to 0.85 gram per cubic meter.

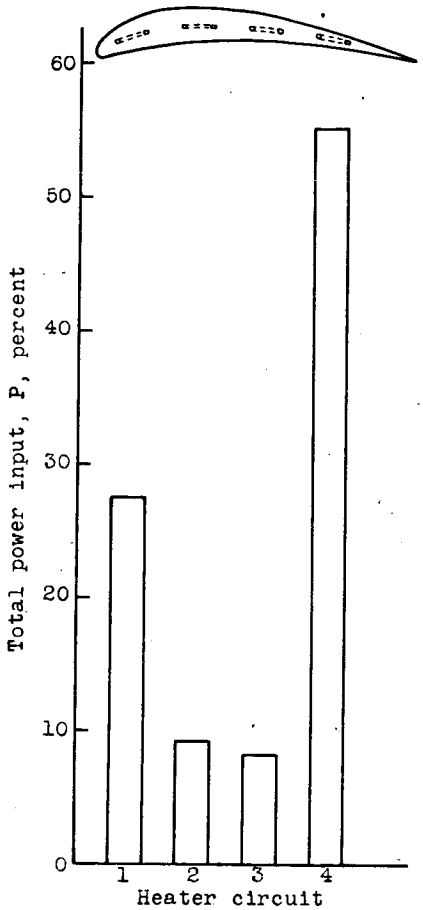

Figure 11. - Minimum average total power per heater for icing protection with continuous heating.

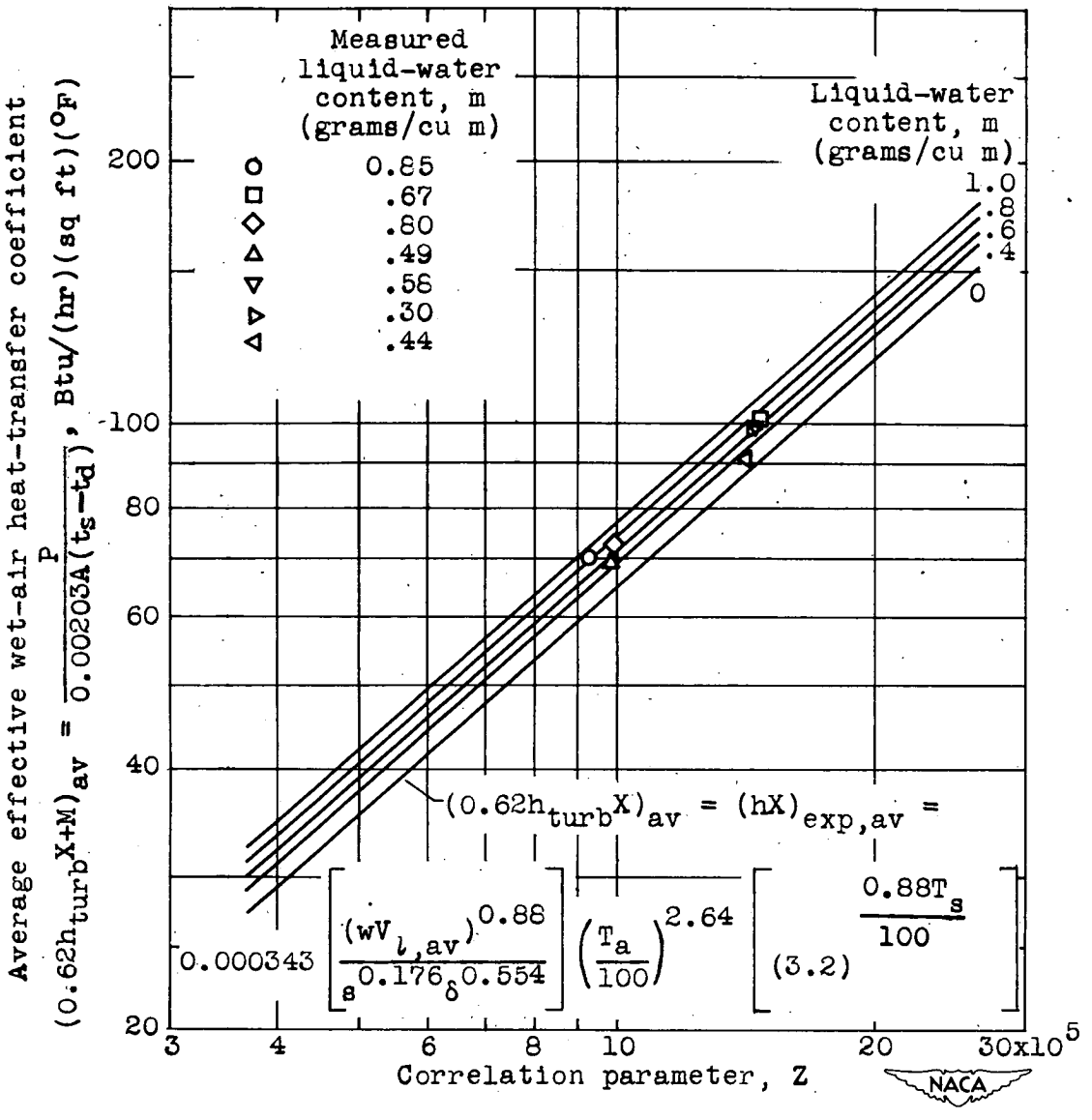

Figure 12. - Correlation of average experimental wet-air heat-transfer coefficients with theoretical values.

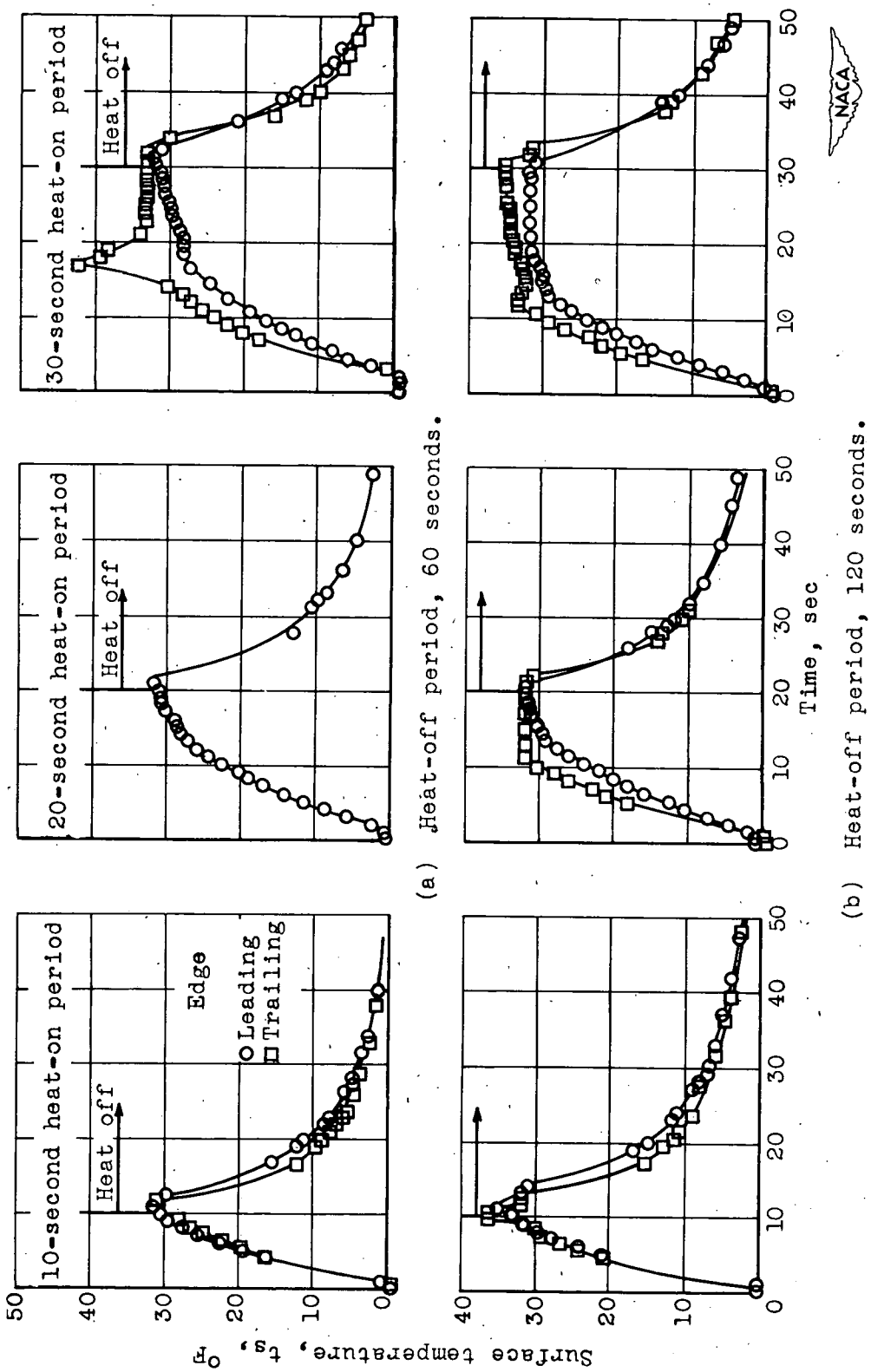

Figure 13. - Typical surface-temperature-rise curves at leading and trailing edges for various heat-on periods as function of time. Air velocity, approximately 392 feet per second; ambient-air temperature, -11° F; liquid-water content, approximately 0.6 gram per cubic meter.

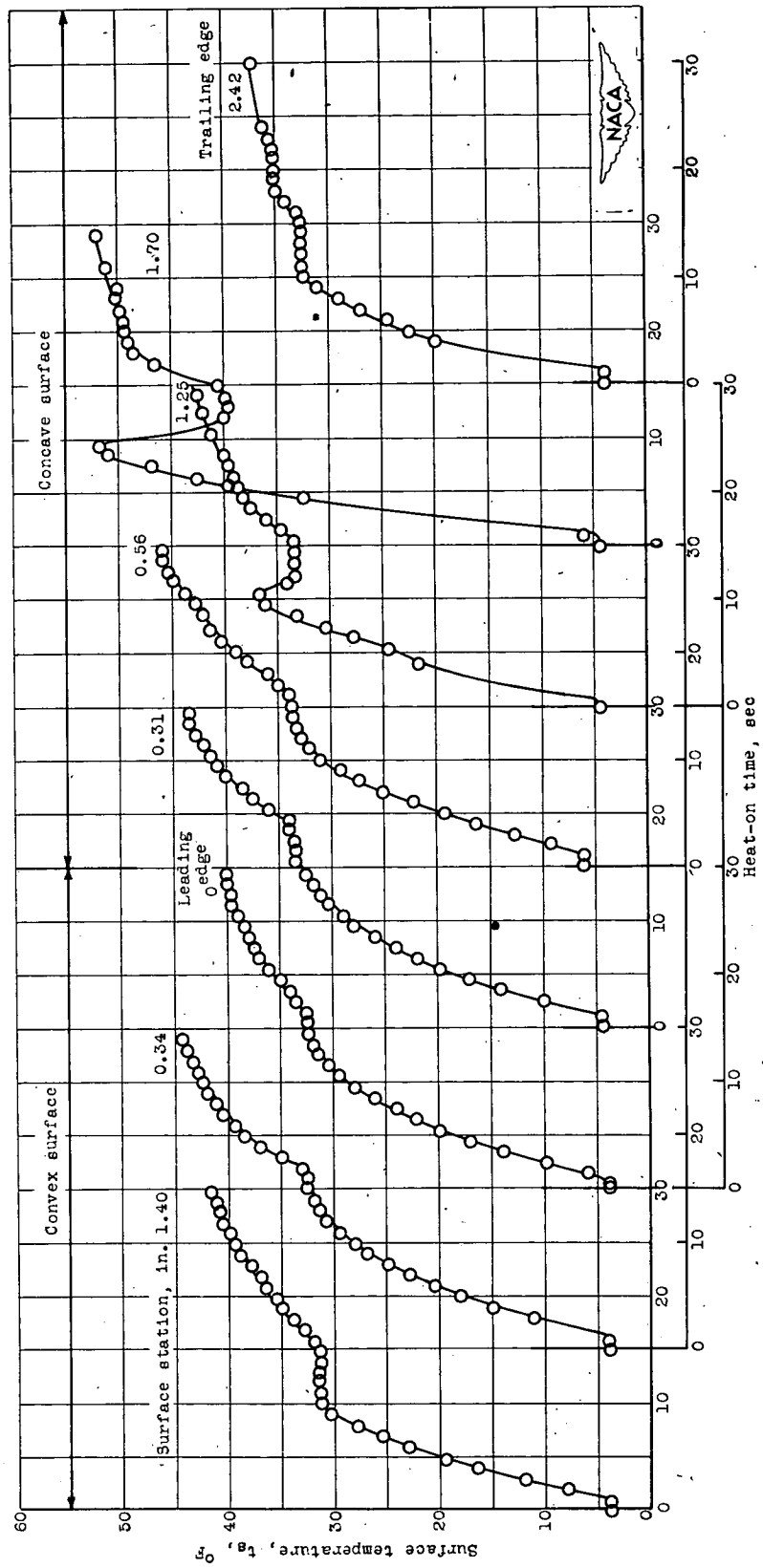

Figure 14. - Typical surface-temperature-rise curves at various surface stations on inlet guide vane as function of time. Complete de-icing of vane with 16-second heat-on period. Air velocity, 392 feet per second; ambient-air temperature, -11° F; liquid-water content, approximately 0.6 gram per cubic meter.

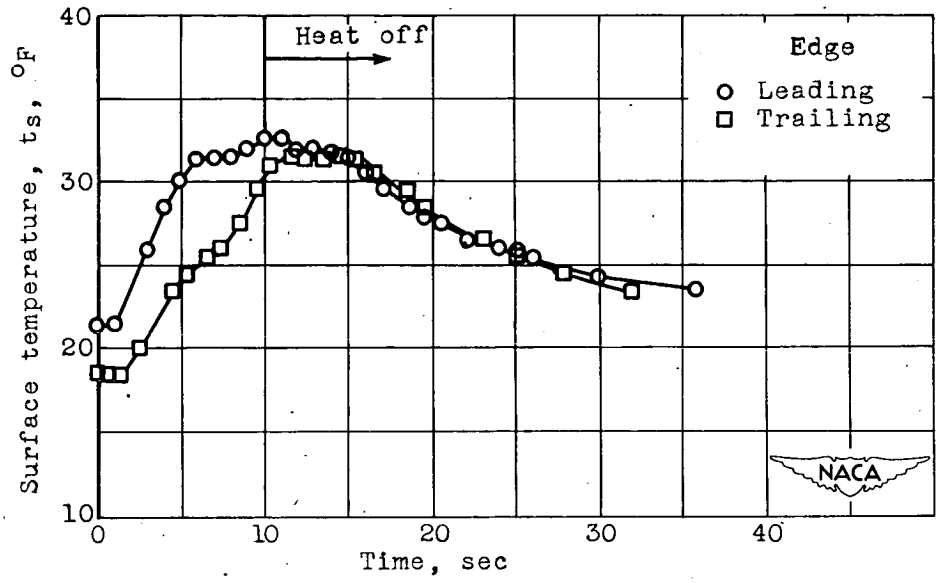

Figure 15. - Typical variation of vane-surface temperature rise with time at ambient-air temperature of 11° F. Air velocity, 383 feet per second; liquid-water content, approximately 0.8 gram per cubic meter; heat-on period, 10 seconds.

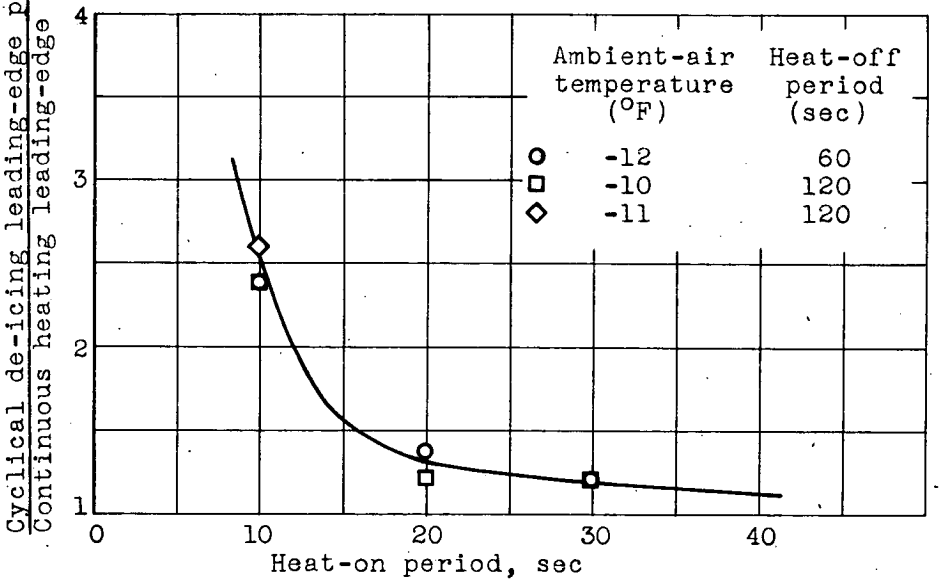

Figure 16. - Ratio of power inputs at leading edge required for cyclical de-icing and for continuous heating as function of heat-on period. Air velocity, approximately 400 feet per second; liquid-water content, approximately 0.6 to 0.8 gram per cubic meter.

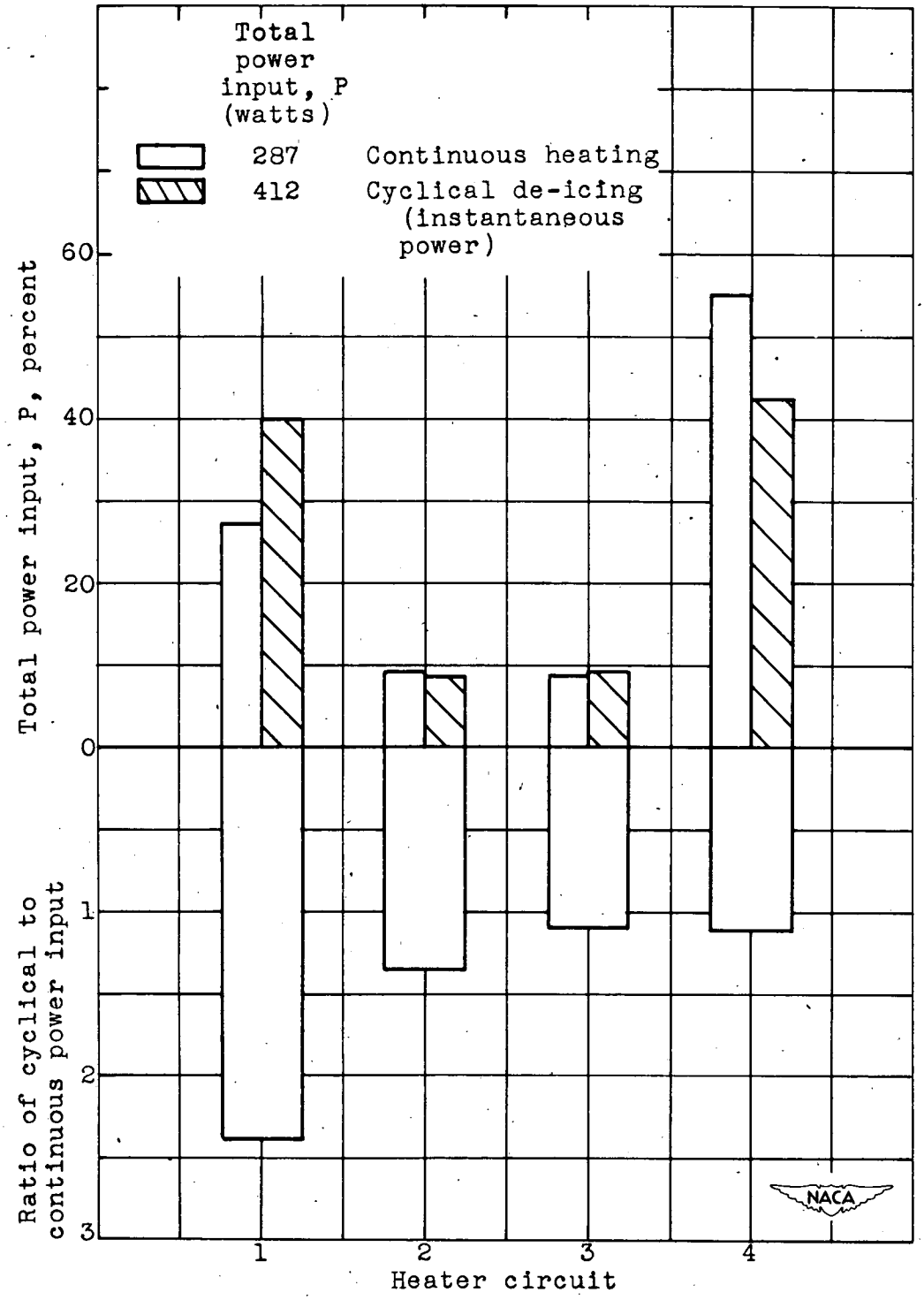

Figure 17. - Comparison of typical power input to individual heaters required for ice protection by cyclical de-icing with 10-second heat-on period and by continuous heating.

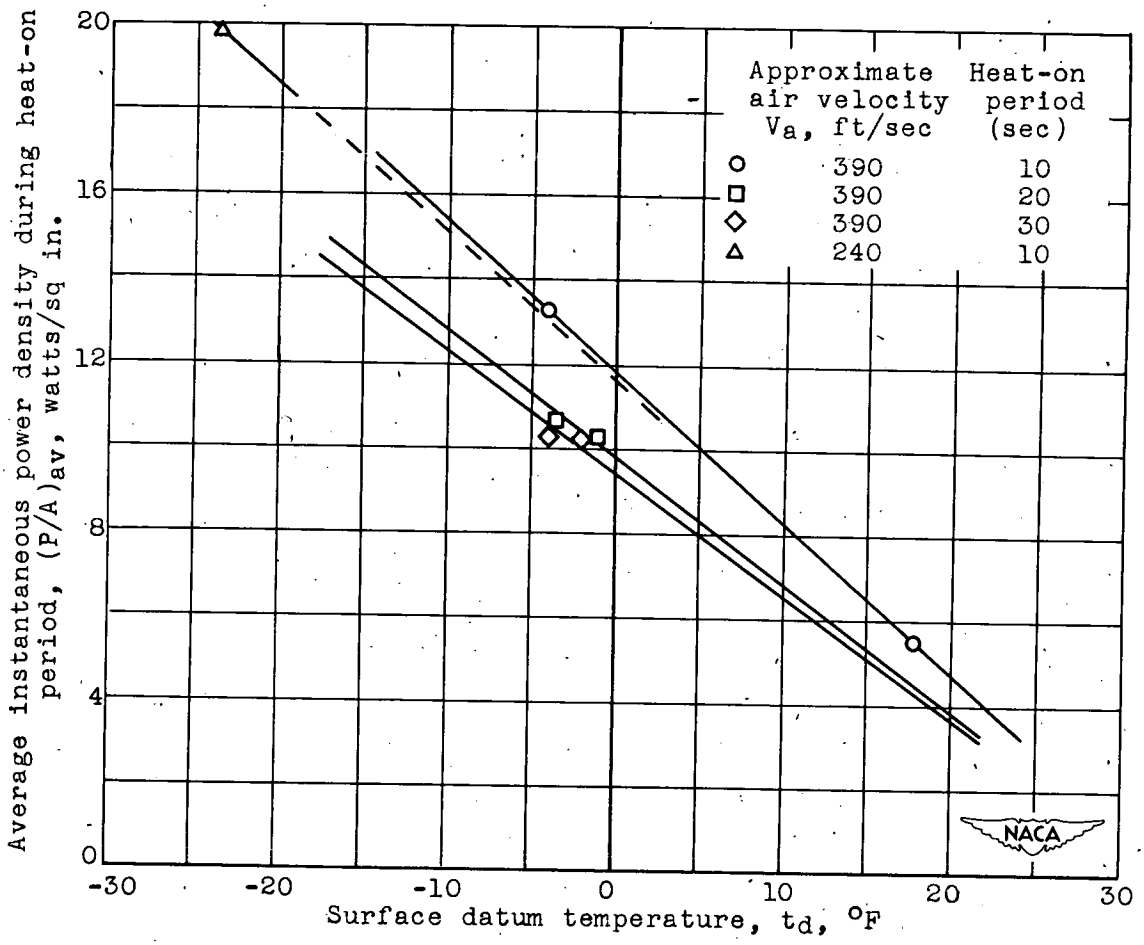

Figure 18. - Evaluation of average instantaneous power density required for ice protection using cyclical de-icing as function of surface datum temperature. Liquid-water content, 0.3 to 0.8 gram per cubic meter; heat-off periods, 60 to 120 seconds.

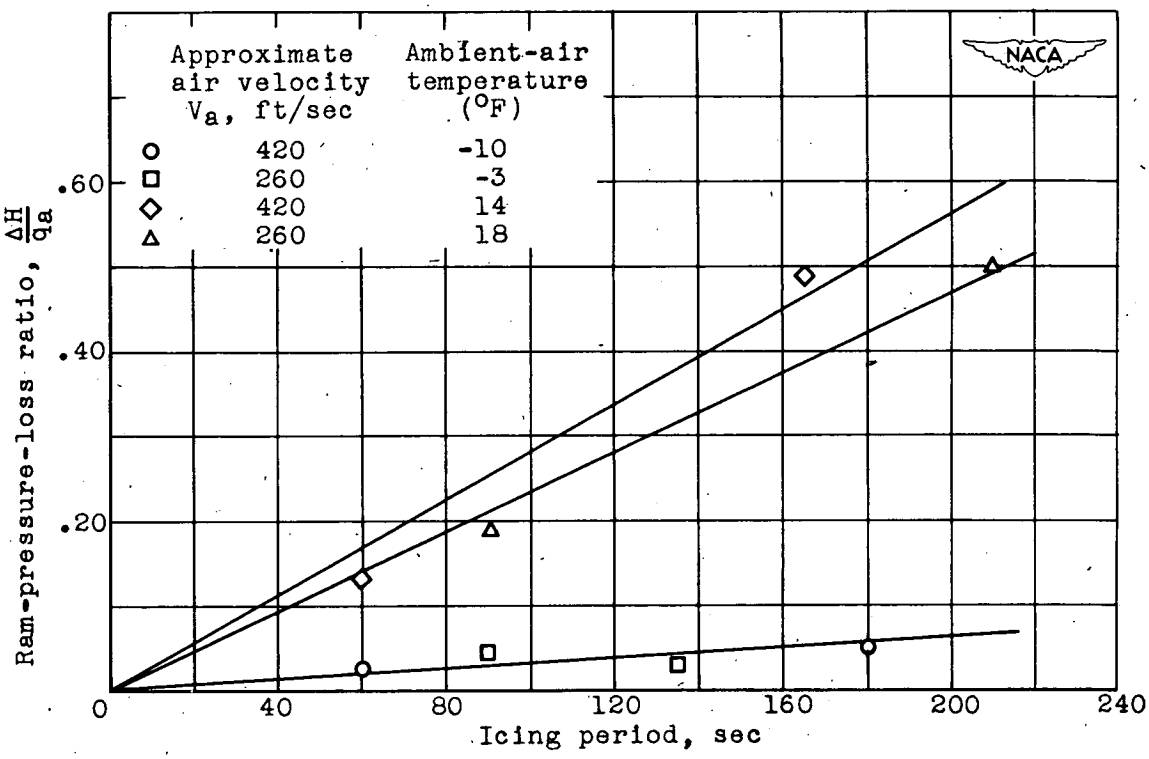

Figure 19. - Effect of ice formations on aerodynamic characteristics of typical inlet guide vanes. Liquid-water content, 0.6 to 0.8 gram per cubic meter.

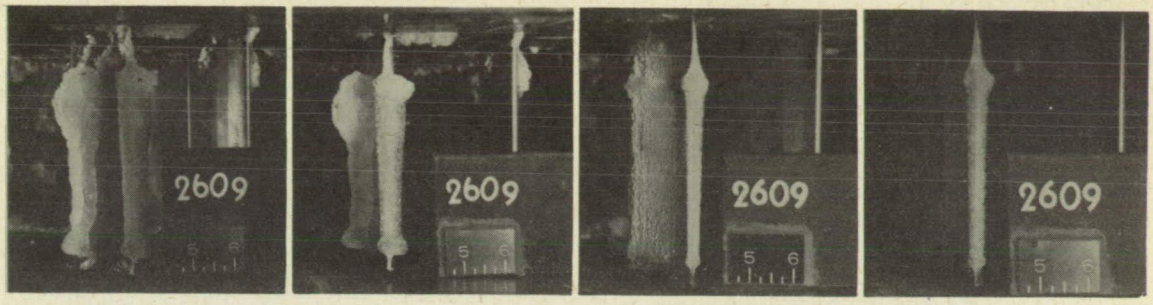

120-second icing period 60-second icing period

(a) Ambient-air temperature, 10° F; liquid-water content, approximately 0.8 gram per cubic meter.

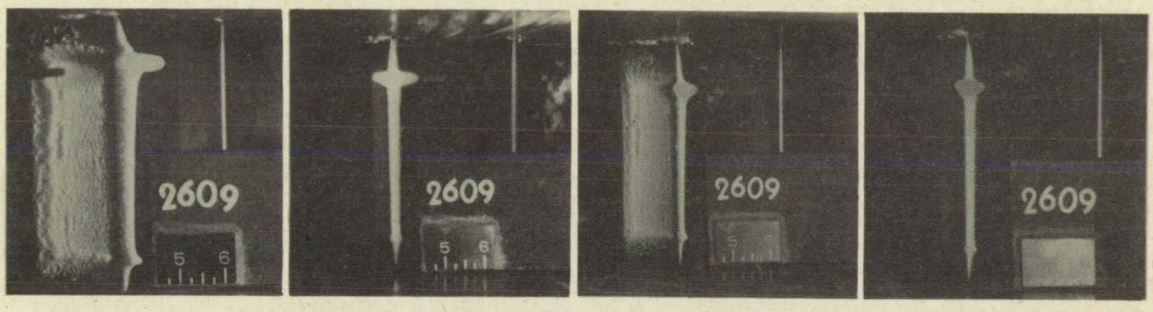

120-second icing period 60-second icing period

(b) Ambient-air temperature, -10° F; liquid-water content approximately 0.6 gram per cubic meter.

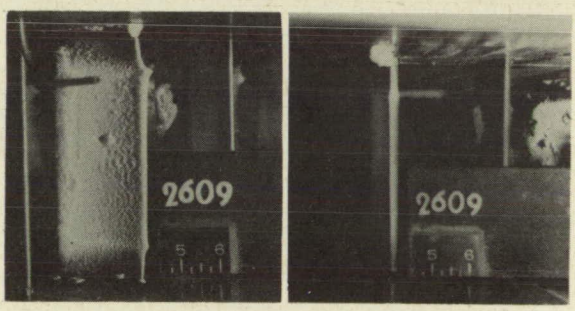

NACA
C-26475

60-second icing period

(c) Ambient-air temperature, -31° F; liquid-water content, approximately 0.4 gram per cubic meter.

Figure 20. - Typical ice formations on inlet guide vane for various icing conditions. Air velocity, approximately 400 feet per second.

Page intentionally left blank

Page intentionally left blank

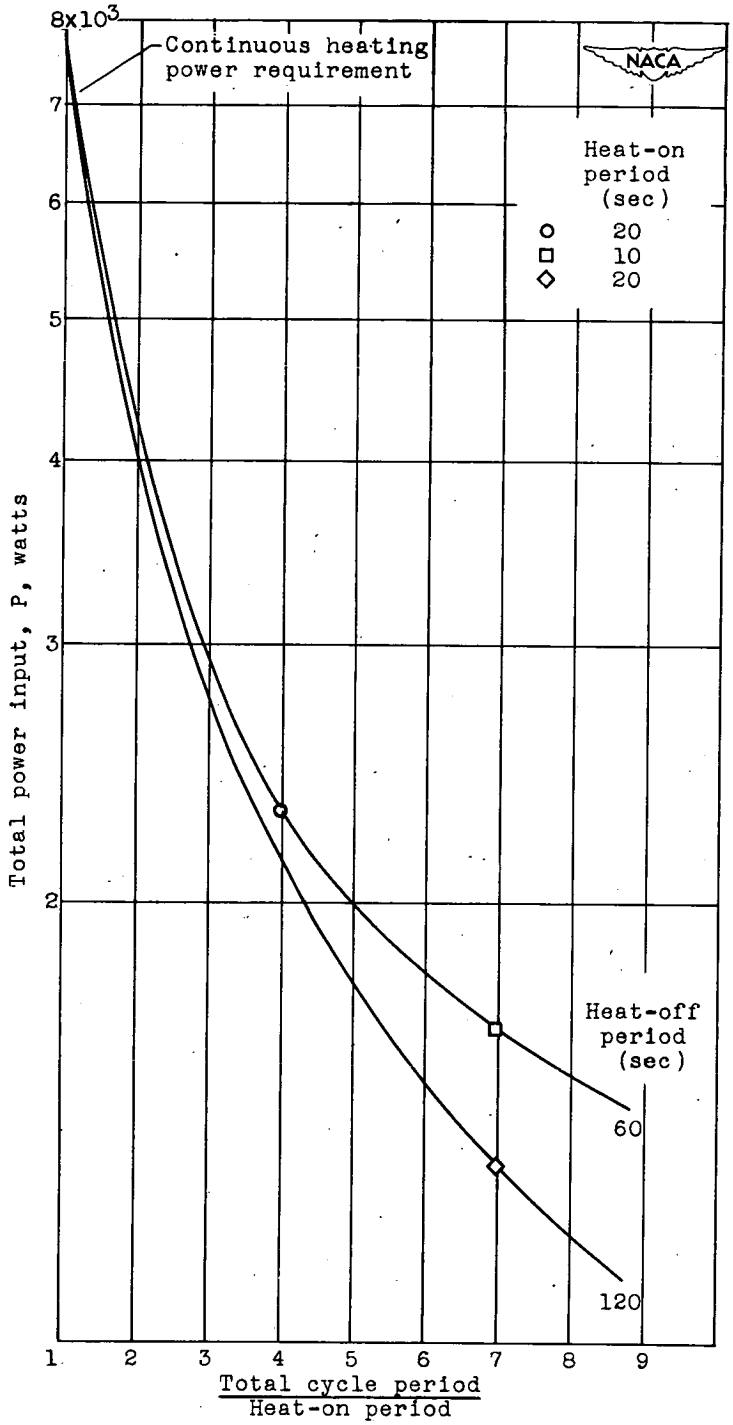

Figure 21. - Total power requirements as function of cycle ratio for cyclical deicing of hypothetical turbojet engine containing 28 double-size inlet guide vanes. Air velocity, 400 feet per second; liquid-water content, approximately 0.6 gram per cubic meter; ambient-air temperature, -11° F.

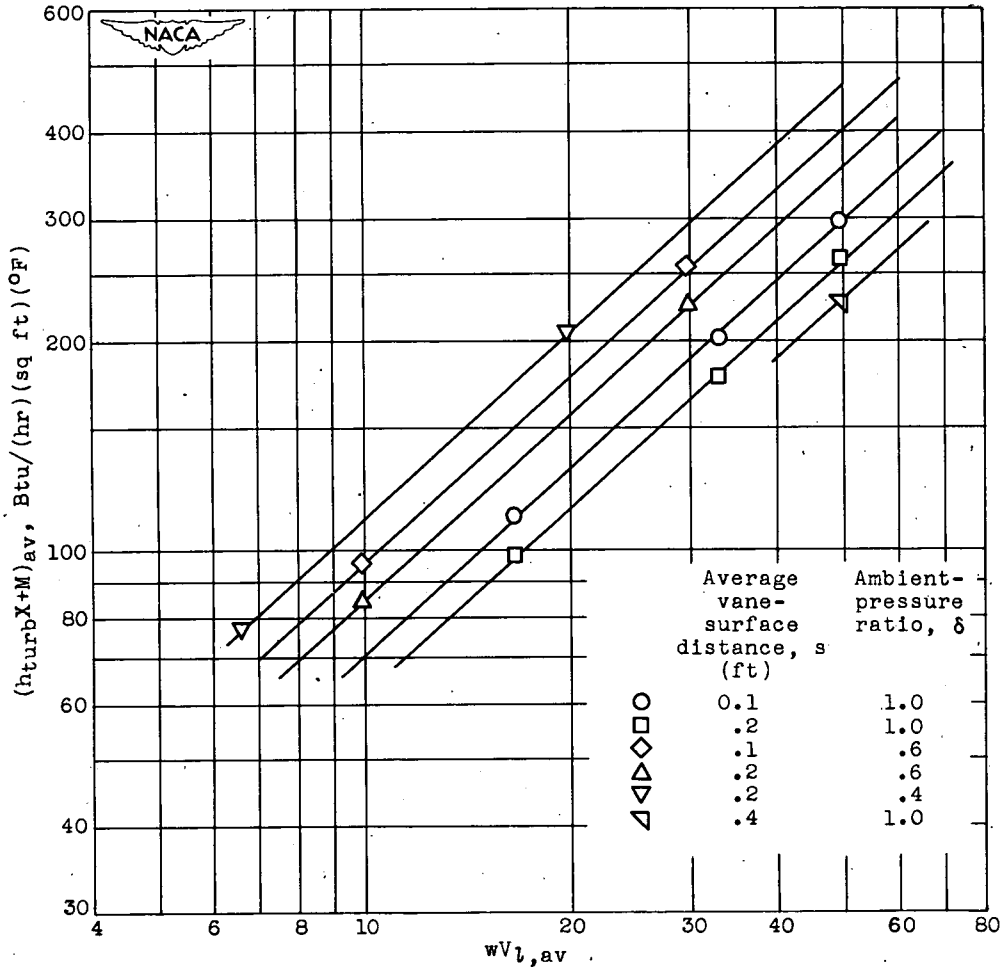

(a) Correlation of $(h_{turb}{}^{XM})_{av}$ with $wV_{l,av}$. Liquid-water content, 1.15 grams per cubic meter; surface temperature, 40° F; absolute ambient-air temperature, 480° R.

Figure 22. - Evaluation of parameter Z for correlating average wet-air heat-transfer coefficient $(h_{turb}{}^{X+M})_{av}$ and average base wet-air heat-transfer coefficient $(h_{turb}{}^{X})_{av}$ on individual curves.

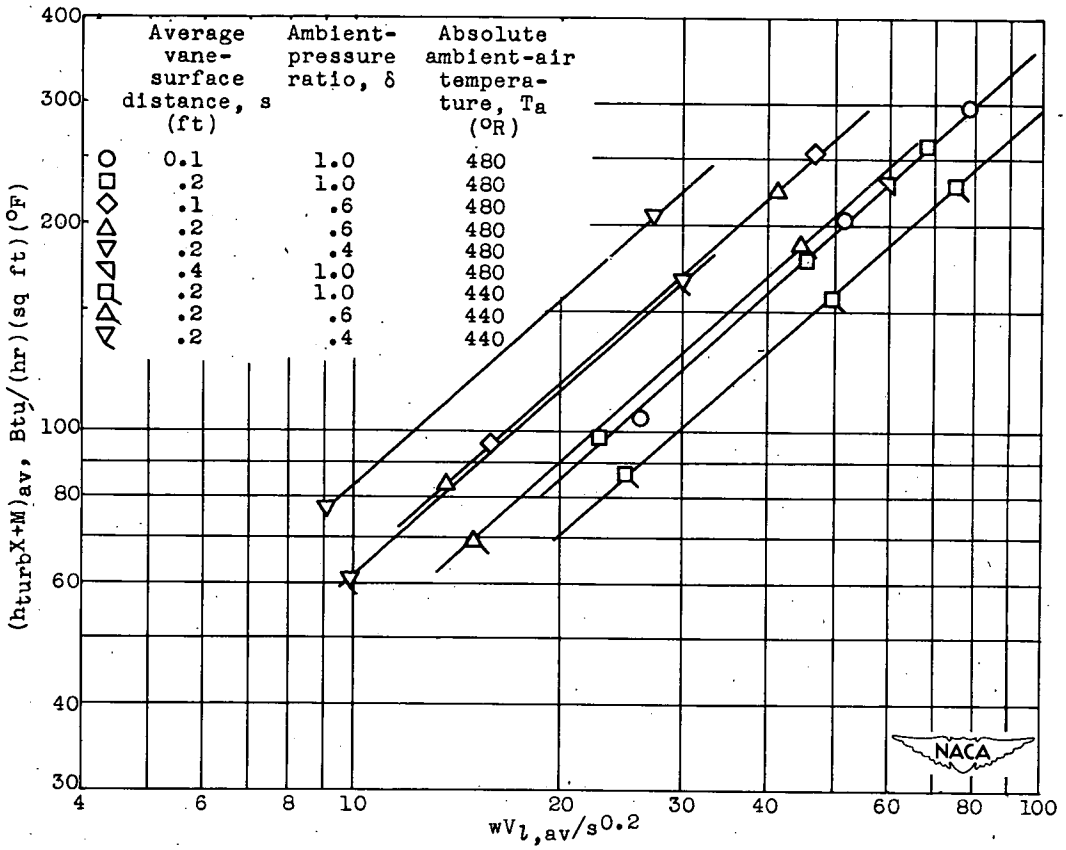

(b) Correlation of $(h_{turb}X+M)_{av}$ with $wV_{l,av}/s^{0.2}$. Liquid-water content, 1.15 grams per cubic meter; surface temperature, 40° F.

Figure 22. - Continued. Evaluation of parameter Z for correlating average wet-air heat-transfer coefficient $(h_{turb}X+M)_{av}$ and average base wet-air heat-transfer coefficient $(h_{turb}X)_{av}$ on individual curves.

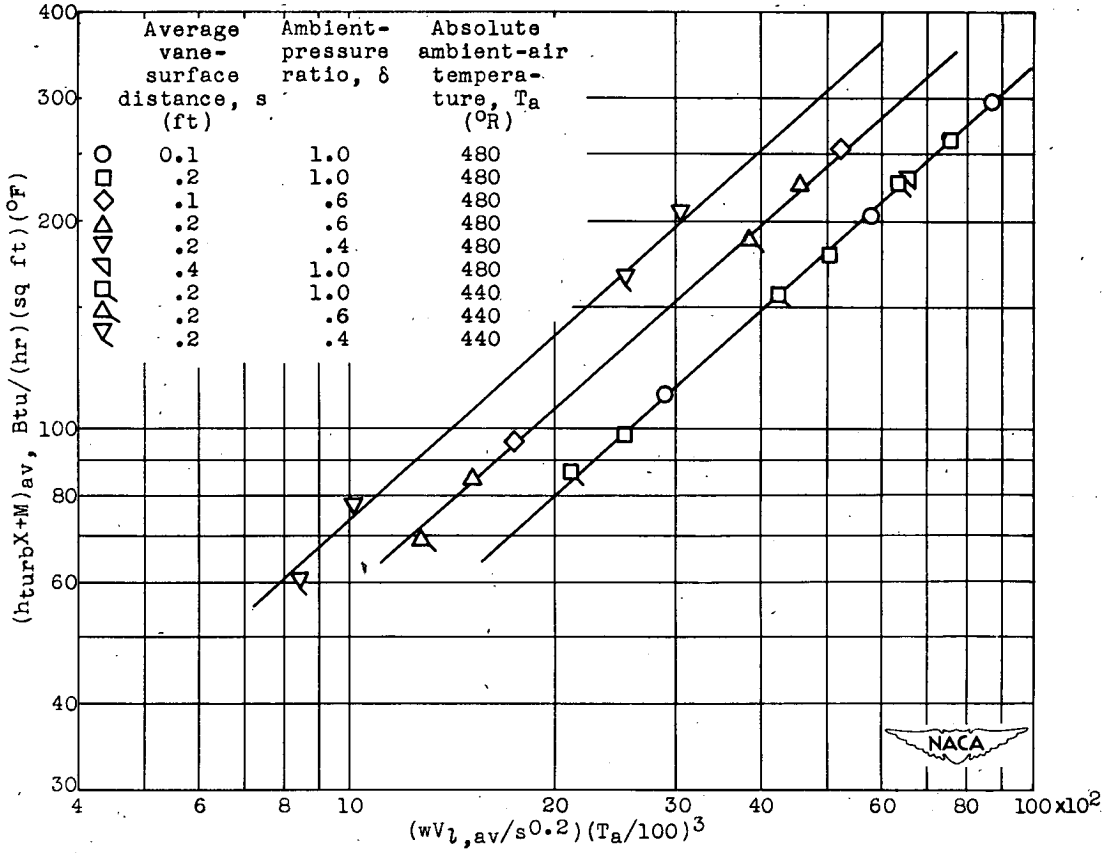

(c) Correlation of $(h_{turb}X+M)_{av}$ with T_a. Liquid-water content, 1.15 grams per cubic meter; surface temperature, 40° F.

Figure 22. - Continued. Evaluation of parameter Z for correlating average wet-air heat-transfer coefficient $(h_{turb}X+M)_{av}$ and average base wet-air heat-transfer coefficient $(h_{turb}X)_{av}$ on individual curves.

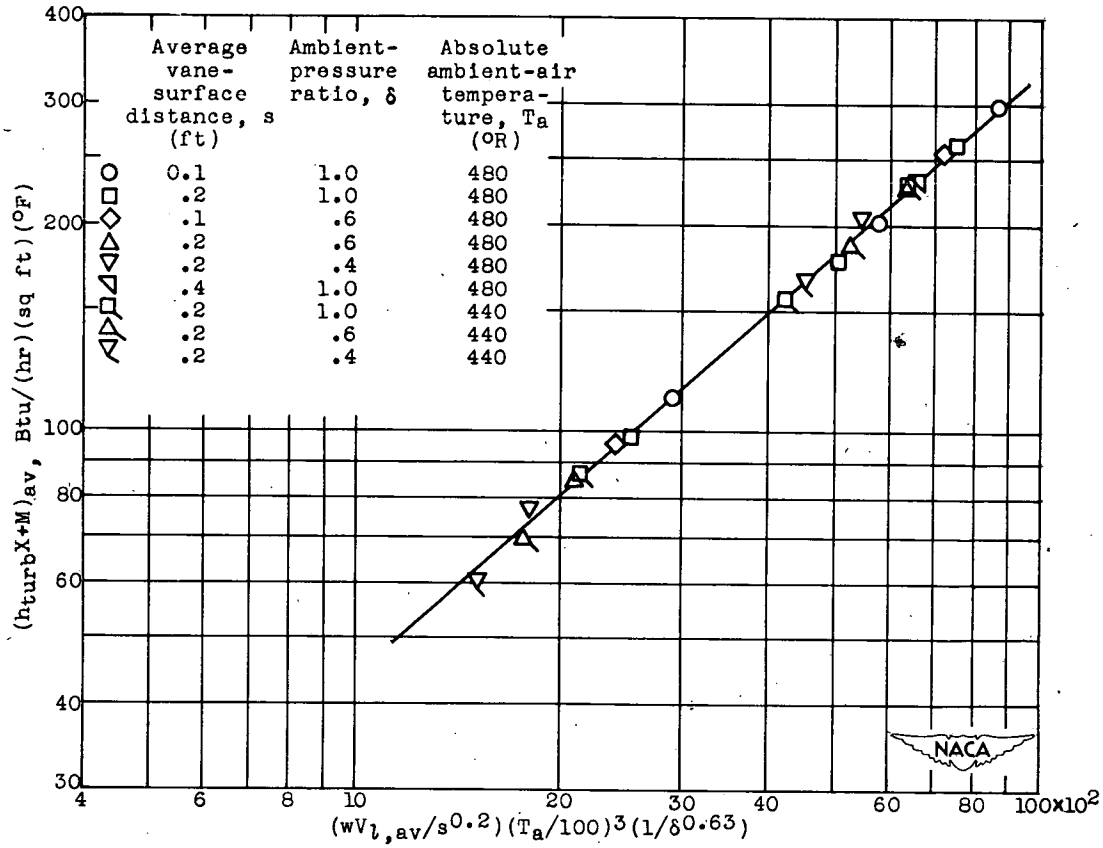

(d) Correlation of $(h_{turbX+M})_{av}$ with δ. Liquid-water content, 1.15 grams per cubic meter; surface temperature, 40° F.

Figure 22. - Continued. Evaluation of parameter Z for correlating average wet-air heat-transfer coefficient $(h_{turbX+M})_{av}$ and average base wet-air heat-transfer coefficient $(h_{turbX})_{av}$ on individual curves.

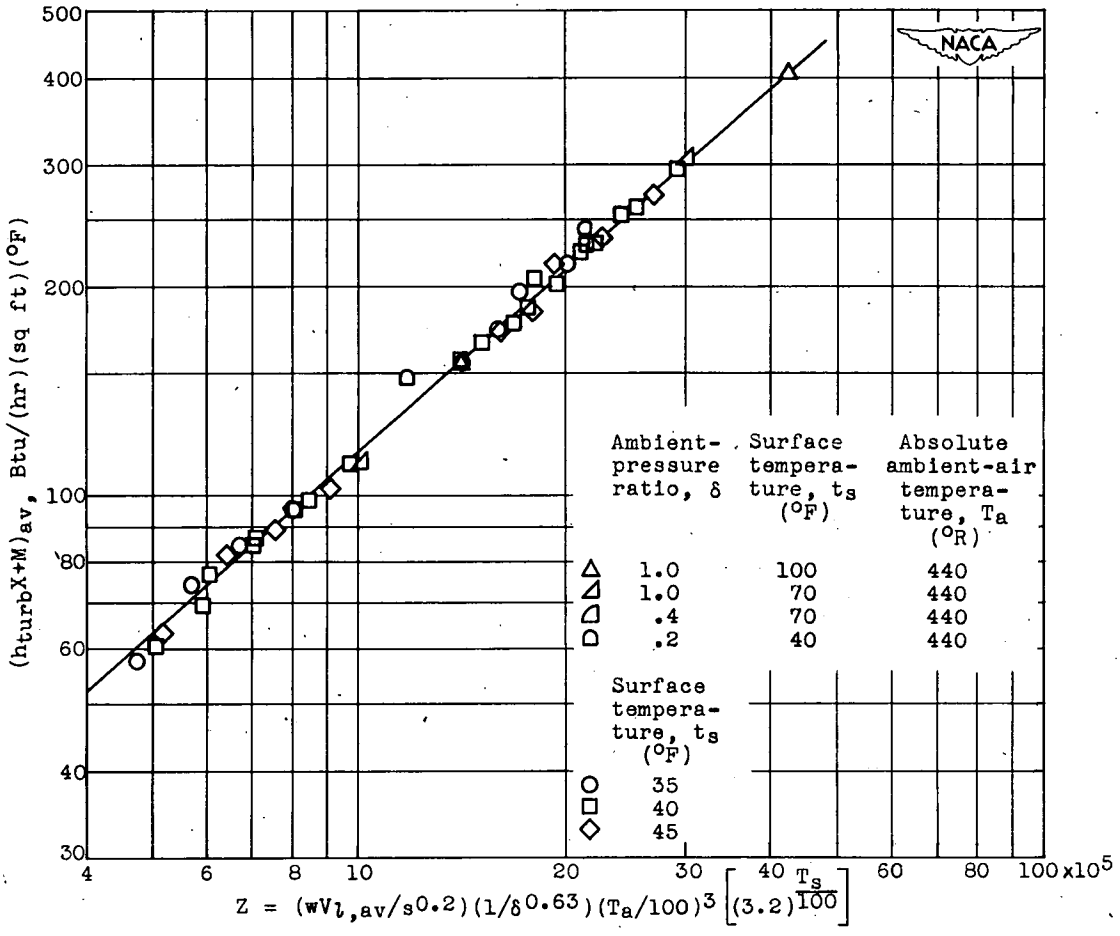

(e) Correlation of $(h_{turb}X+M)_{av}$ with t_s and with Z. Liquid-water content, 1.15 grams per cubic meter.

Figure 22. - Continued. Evaluation of parameter Z for correlating average wet-air heat-transfer coefficient $(h_{turb}X+M)_{av}$ and average base wet-air heat-transfer coefficient $(h_{turb}X)_{av}$ on individual curves.

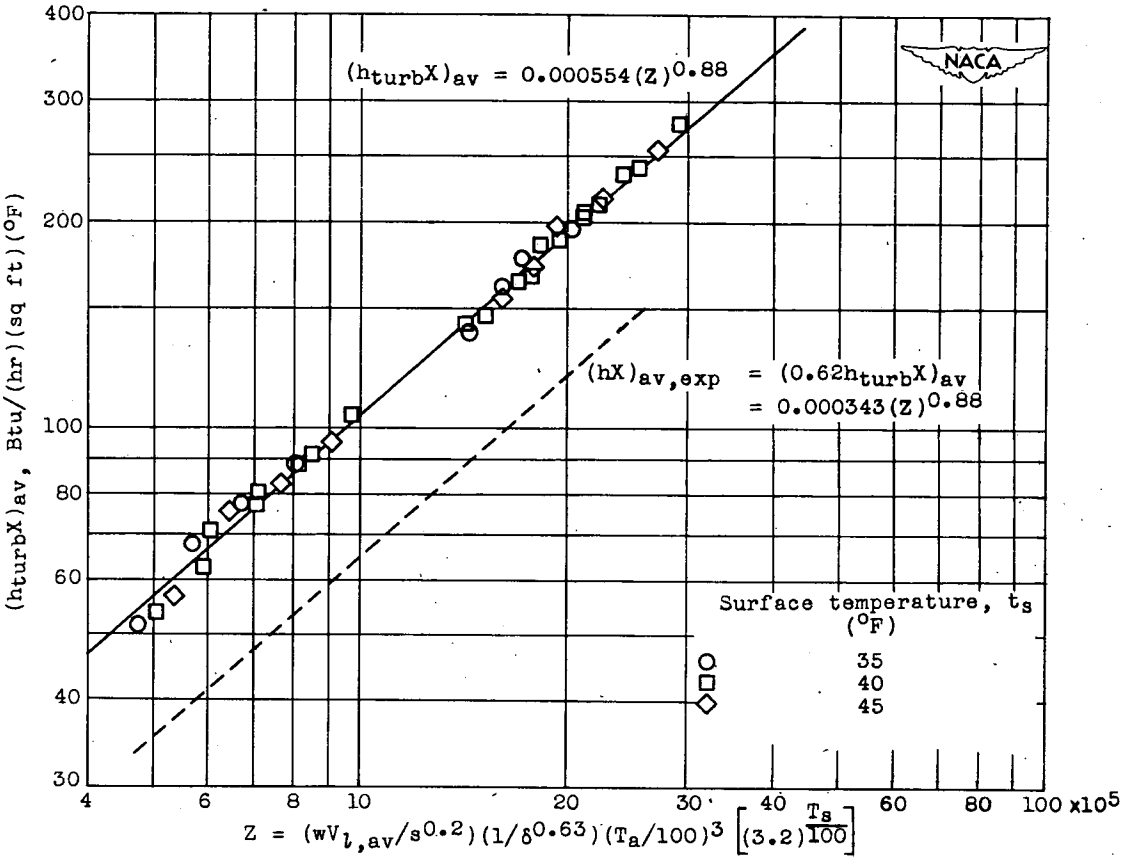

(f) Correlation of $(h_{turbX})_{av}$ with Z. Liquid-water content, 0 gram per cubic meter; surface temperature, 40° F.

Figure 22. - Concluded. Evaluation of parameter Z for correlating average wet-air heat-transfer coefficient $(h_{turbX+M})_{av}$ and average base wet-air heat-transfer coefficient $(h_{turbX})_{av}$ on individual curves.